TAMPEREEN TEKNILLINEN YLIOPISTO
TAMPERE UNIVERSITY OF TECHNOLOGY

ILMO HEISKA

SIMULATION OF A COMBINED CYCLE PROCESS WITH OXYFUEL COMBUSTION AND CARBON CAPTURE

Master of Science Thesis

Examiner: D.Sc. Henrik Tolvanen
Examiner and topic approved by the Faculty Council of the Faculty of Natural Sciences on 5 October 2016

ABSTRACT

ILMO HEISKA: Simulation of a Combined Cycle Process with Oxyfuel Combustion and Carbon Capture
Tampere University of Technology
Master of Science Thesis, 72 pages
October 2016
Master's Degree Programme in Environmental and Energy Engineering
Major: Power Plants and Combustion Technology
Examiner: D.Sc. Henrik Tolvanen

Keywords: argon, Aspen Plus, carbon capture, combined cycle, oxyfuel combustion, process simulation

The aim of this thesis was to present a combined cycle process with oxyfuel combustion and carbon capture and to study the process through simulation. Two different cases were used to study the effect of a working fluid with and without argon for the process. The thesis includes studying the concept of a combined cycle process and its basic processes, the simulation of the two cases using Aspen Plus simulation software and the analysis of the results with comparison to a similar process, the Graz Cycle.

The simulation model was built according to a patent application by Dr. Matti Nurmia for a Brayton-Rankine process with carbon capture. Case 1 was used for the process without argon and Case 2 for the process with argon. The model configuration and parameters used for the two cases had only minor differences in order to get as comparable results as possible. The completed model was optimized for both cases using the optimization tool of Aspen Plus.

The simulation results showed that the thermal efficiency of the process was 0.565 for Case 1 and 0.535 for Case 2. The separation of carbon dioxide from the process is more straightforward for Case 1 but for Case 2 the separation of carbon dioxide from a mixture consisting mainly of argon and carbon dioxide requires energy. When the energy required for oxygen supply was estimated for both cases as well as the separation work for Case 2, the net efficiency of the process was determined as 0.539 for Case 1 and 0.506 for Case 2, while the net efficiency for the Graz Cycle was 0.548. The pressure ratio for the main gas turbine in the process was determined as 87.0 in Case 1 and 20.8 in Case 2 which was caused by lower discharge pressure in Case 1 as the main gas turbine inlet pressure was the same for both cases. The discharge pressure for the main gas turbine was determined as 0.230 bar in Case 1 and 0.936 bar in Case 2. The results indicate that the use of argon in such a combined cycle could have major benefits as a lower pressure ratio on one hand and a higher discharge pressure on the other hand should lead to capital cost savings considering the structure of the main gas turbine and the heat recovery steam generator of the process.

Further research on the separation of carbon dioxide from a mixture consisting mainly of argon and carbon dioxide is suggested. A more complete economic analysis of the process and a demo-scale plant are recommended to verify the results and confirm the economic feasibility of the process as well as find out which one of the two simulated cases could provide more cost-effective results in practice.

TIIVISTELMÄ

ILMO HEISKA: Kombivoimaprosessin simulointi happipoltolla ja hiilen talteenotolla
Tampereen teknillinen yliopisto
Diplomityö, 72 sivua
Lokakuu 2016
Ympäristö- ja energiatekniikan diplomi-insinöörin tutkinto-ohjelma
Pääaine: Voimalaitos- ja polttotekniikka
Tarkastaja: Tekniikan tohtori Henrik Tolvanen

Avainsanat: argon, Aspen Plus, happipoltto, hiilen talteenotto, kombivoimaprosessi, prosessisimulointi

Tämän työn tarkoituksena oli esitellä eräs happipolttoa käyttävä kombivoimaprosessi hiilen talteenotolla sekä tämän prosessin simuloiminen. Työssä käytettiin kahta erilaista tapausta (Case 1 ja Case 2), jotta voitiin tutkia argonin mukanaoloa työaineessa ja sen vaikutusta prosessiin. Tämä työ sisältää kombivoimaprosessin konseptin ja sen perusprosessien esittelyn, kahden tapauksen simuloinnin Aspen Plus -ohjelmistolla sekä saatujen tulosten analysoinnin ja vertailun vastaavaan Graz Cycle -prosessiin.

Simulaatiomalli muodostettiin tohtori Matti Nurmian patenttihakemuksessa esitetyn Brayton-Rankine prosessin mukaisesti. Tapaus Case 1:n simulointia käytettiin prosessin tutkimiseen ilman argonia ja tapaus Case 2:n simulointia käytettiin prosessin tutkimiseen argonin kanssa. Simulointimallit ja niissä käytetyt parametrit sisälsivät vain vähän eroavaisuuksia, jotta tulokset olisivat mahdollisimman vertailukelpoiset keskenään. Valmiit simulaatiomallit optimoitiin Aspen Plus -ohjelmiston optimointityökalun avulla.

Simulaatiotulosten mukaan kombivoimaprosessin termiseksi hyötysuhteeksi saatiin 0,565 Case 1:n tapauksessa ja 0,535 Case 2:n tapauksessa. Hiilidioksidin erottaminen prosessista on suoraviivaisempaa Case 1:n tapaukselle, mutta Case 2:n tapauksessa hiilidioksidin erottamiseen argonin ja hiilidioksidin seoksesta tarvitaan työtä. Kun hapen tuotantoon tarvittava energia arvioitiin molemmille tapauksille ja lisäksi hiilidioksidin erotustyö tapaukselle Case 2, saatiin prosessin nettohyötysuhteeksi 0,539 tapaukselle Case 1 ja 0,506 tapaukselle Case 2, kun taas nettohyötysuhde Graz Cycle -prosessille oli 0,548. Prosessin pääkaasuturbiinin painesuhteeksi saatiin 87,0 tapaukselle Case 1 ja 20,8 tapaukselle Case 2, mikä johtui alemmasta paisuntapaineesta tapauksessa Case 1, sillä turbiinin alkupaine oli molemmissa tapauksissa sama. Pääkaasuturbiinin paisuntapaineeksi saatiin 0,230 bar tapaukselle Case 1 ja 0,936 bar tapaukselle Case 2. Nämä tulokset viittaavat siihen, että argonin käyttö esitetyssä kombivoimaprosessissa voisi mahdollistaa merkittäviä etuja, sillä pienemmän painesuhteen ja korkeamman paisuntapaineen pitäisi johtaa merkittäviin säästöihin kiinteissä kustannuksissa prosessin kaasuturbiinin ja lämmönsiirtimen rakenteen takia.

On suositeltavaa, että hiilidioksidin erottamista argonin ja hiilidioksidin seoksesta tutkittaisiin tarkemmin. Tarkempaa taloudellista tarkastelua ja demolaitosta suositellaan, jotta voidaan vahvistaa työssä saadut tulokset ja varmistaa esitetyn prosessin taloudellinen toteutettavuus sekä selvittää kumpi kahdesta simulointitapauksesta osoittautuisi kustannustehokkaammaksi käytännössä.

PREFACE

First of all I would like to thank Risto Raiko for providing me with the opportunity to work on this thesis. I would also like to thank my examiner Henrik Tolvanen and Matti Nurmia for their valuable comments and advice regarding this thesis.

Finally, I am grateful for all the support I have received during my studies. I would like to express my gratitude towards my parents for supporting me from day one; my brothers for their continuous support; and my friends at TUT for peer support during studies and the countless lunch and coffee breaks.

Tampere, 28.10.2016

Ilmo Heiska

CONTENTS

1. INTRODUCTION 1
2. GAS AND STEAM TURBINE CYCLES FOR POWER GENERATION 3
2.1 Gas turbine cycle 5
2.1.1 Brayton cycle 6
2.1.2 Unit processes 10
2.1.3 Methods for improving efficiency 13
2.2 Steam turbine cycle 15
2.2.1 Rankine cycle 16
2.2.2 Unit processes 17
2.2.3 Methods for improving efficiency 18
2.3 Combined cycle 21
2.3.1 Configuration 22
2.3.2 Unit processes 22
2.3.3 Methods for improving efficiency 24
3. WORKING FLUIDS IN GAS AND STEAM TURBINE CYCLES 26
3.1 Gas turbine cycles 26
3.2 Steam turbine cycles 29
4. CARBON CAPTURE IN POWER GENERATION 32
4.1 Pre-combustion capture 33
4.2 Post-combustion capture 33
4.3 Oxyfuel combustion 33
5. INTRODUCTION TO ASPEN PLUS 36
5.1 Initial specifications for simulation 37
6. PROCESS SIMULATION 40
6.1 Process description 40
6.2 Simulated cases 42
6.2.1 Case 1 43
6.2.2 Case 2: with argon 45
6.3 Process specifications for the simulation 47
6.4 Optimization 50
6.5 Component modelling in Aspen Plus 51
6.6 Problems 57
7. RESULTS AND DISCUSSION 58
8. CONCLUSIONS 69
REFERENCES 71

LIST OF FIGURES

Figure 1. *The Carnot cycle on a temperature-entropy diagram. [5]* *4*

Figure 2. *A simple gas turbine cycle. [5]* *5*

Figure 3. *An illustration of a single-shaft gas turbine. [8]* *6*

Figure 4. *An ideal Brayton cycle. [5]* *7*

Figure 5. *Temperature-entropy diagram (left) and pressure-volume diagram (right) for an ideal Brayton cycle. [5]* *8*

Figure 6. *Actual and isentropic compression and actual and isentropic expansion for a Brayton cycle. [5]* *9*

Figure 7. *Actual and ideal thermal efficiency (left) and actual and ideal net work (right) for a Brayton process when $\eta_t = 0.85$, $\eta_c = 0.8$, $T_3 = 1200$ K and $T_1 = 300$ K. Adapted from [5]* *10*

Figure 8. *Enthalpy changes in the impeller and nozzle sections of a turbine. The actual enthalpy changes are marked with $\Delta h'$ and $\Delta h''$ for nozzle section and impeller section, respectively. Isentropic enthalpy changes are marked with the subscript 's'. [9]* *12*

Figure 9. *A simple open loop gas turbine cycle with heat regeneration (left), adapted from [5]. Heat regeneration on a temperature-entropy diagram (right).* *13*

Figure 10. *Intercooling in a Brayton cycle on a temperature-entropy diagram. Sub-processes 1-2 and 3-4 express compression and sub-process 2-3 expresses intercooling.* *14*

Figure 11. *A schematic (left) and a temperature-entropy diagram (right) of reheating. Adapted from [10]* *15*

Figure 12. *A basic steam turbine cycle. [7]* *16*

Figure 13. *A temperature-entropy diagram of a Rankine cycle. The temperature increase in the sub-process 1-2 is overemphasized for illustration purposes. [7]* *17*

Figure 14. *Thermal efficiency of a Rankine cycle as a function of inlet temperature, when condenser pressure is $p_2 = 0.04$ bar (left) and the effect of superheating on a temperature-entropy diagram (right). Adapted from [12]* *19*

Figure 15. *The effect of increasing the turbine inlet pressure on a Rankine cycle on a temperature-entropy diagram (left) and the thermal efficiency as a function of turbine inlet pressure when turbine outlet pressure is $p_2 = 0.4$ bar (right). Adapted from [12]* *20*

Figure 16. *The thermal efficiency as a function of turbine outlet pressure (left) and the effect of lowering the turbine outlet pressure on a temperature-entropy diagram (right) on a Rankine cycle. Adapted from [12].* *20*

Figure 17. *The effect of steam reheating on a Rankine cycle on a temperature-entropy diagram.[12] 21*
Figure 18. *The schematic of a basic combined cycle. 22*
Figure 19. *The temperature-entropy diagram of a combined cycle process where Brayton cycle is used as the topping cycle and Rankine cycle is used as the bottoming cycle. 24*
Figure 20. *The liquid-vapor critical point on a pressure-temperature diagram.[18] 30*
Figure 21. *Simplified situation for the phase change from liquid to steam (left) and the transition to supercritical steam (right) for water. The transition to supercritical steam is drawn according to [16]. 30*
Figure 22. *Methods for CO_2 capture from power generation. [19] 32*
Figure 23. *Simplified process flowsheet for the simulated process. 41*
Figure 24. *The process flowsheet for Case 1. ..... 44*
Figure 25. *The process flowsheet for Case 2. The difference between Case 1 and Case 2 process flowsheets is highlighted in yellow. 46*
Figure 26. *The Compr block setup window. 53*
Figure 27. *Case 1: the transition to supercritical steam in the middle section of the HRSG. T_HOT depicts the combustion gases and T_COLD depicts the recirculation water. The recirculation water at pressure p = 300 bar. 62*
Figure 28. *Case 2: the transition to supercritical steam in the middle section of the HRSG. T_HOT depicts the combustion gases and T_COLD depicts the recirculation water. The recirculation water at pressure p = 300 bar. 63*

LIST OF SYMBOLS AND ABBREVIATIONS

Term	Explanation	Unit
a	Peng-Robinson equation coefficient	$(kg\ m^5)/(mol^2\ s^2)$
b	Peng-Robinson equation coefficient	m^3/mol
c_p	specific heat at constant pressure	J/(kg K)
c_v	specific heat at constant volume	J/(kg K)
f	degree of freedom	-
h	specific enthalpy	J/kg
k	Peng-Robinson equation coefficient	-
m	mass	kg
$\dot{m}$	mass flow	kg/s
$\dot{n}$	molar flow	mol/s
p	pressure	Pa, bar
P	power	W
Q	heat	W
r	degree of reaction	-
R_u	ideal gas constant	J/(mol K)
s	specific entropy	J/(kg K)
S	entropy	J/K
T	temperature	K, °C
V_m	molar volume	m^3/mol
W	work	W
α	dimensionless constant	-
κ	ratio of specific heats	-
η	efficiency	-
Π	pressure ratio	-
v	specific volume	m^3/kg
ω	acentric factor	-
CCS	carbon capture and storage	
HHV	higher heating value	
HRSG	heat recovery steam generator	
ORC	organic Rankine cycle	

1. INTRODUCTION

In 2010 the European Union member states committed to a Europe 2020 strategy which states three main objectives for climate and energy policy to be reached by 2020:

- reducing the greenhouse gas emissions by at least 20 % compared to 1990 levels,
- moving towards improving energy efficiency by 20 %,
- increasing the share of renewable energy in final energy consumption to 20 %.[1]

Between 1990 and 2014 the greenhouse gas emissions in EU were reduced by all sectors other than fuel combustion in transport and international aviation. In 2014 the greenhouse gas emissions in EU were already down by 23 % compared to the levels in 1990 so EU is likely to exceed the Europe 2020 target of reducing greenhouse gas emissions by 20 % by 2020. Nevertheless, the efforts for further reducing the greenhouse gas emissions and increasing energy efficiency are vital in global scale: the average global surface temperature keeps rising and 2015 was the warmest year on record. [1] In 2014 the EU member states agreed on a new 2030 Framework for climate and energy which provides targets for the period between 2020 and 2030. The 2030 Framework targets include reducing the greenhouse gas emissions by at least 40 % compared to the levels in 1990 and moving towards improving energy efficiency by at least 27 %. [2] The combination of EU wide policies and the fact that greenhouse gas emissions have to be reduced in global scale in order to try to control global warming make it essential to further develop more efficient ways of energy generation and technologies for reducing emissions.

One way of reducing greenhouse gas emissions is carbon capture and storage (CCS). CCS is a concept used to depict a wide range of technologies which are used to prevent or reduce carbon dioxide emissions caused by the combustion of fossil fuels, or any other carbon based fuels. CCS technologies include pre-combustion capture, post-combustion capture and oxyfuel combustion. A combination of carbon capture technologies and more efficient energy generation methods could be an important part of the solution when reaching for the targets set by the EU strategies Europe 2020 and 2030 Framework. At the same time carbon capture technologies and more efficient energy generation methods will most likely play a major role in reducing the impact of greenhouse gas emissions in the battle against global warming.

Oxyfuel combustion is one of the most promising technologies for decreasing carbon dioxide emissions from power plants. Oxyfuel combustion is characterized by burning the fuel in pure or high concentration oxygen instead of air. Oxyfuel combustion leads to

flue gases with high concentration of carbon dioxide and steam which then allows the separation of carbon dioxide with simple condensation process. [3]

The objective of this thesis is to simulate a novel configuration of the combined cycle process. The simulated process is characterized by oxyfuel combustion enabling effective carbon capture from the process, as well as unconventional working fluids and the use of supercritical steam in the steam side of the combined cycle process. The simulation is divided into two cases: Case 1 and Case 2. Case 1 is based on the novel configuration of the combined cycle process with a working fluid consisting mainly of carbon dioxide and steam. A different working fluid is used in Case 2 and the effect of using argon as part of the working fluid is studied. No other major differences exist between the cases. The two-case approach enables studying the novel configuration of the combined cycle process in itself as well as the comparison between the two cases and the effect of argon to the process.

The thesis begins with introducing the basic thermodynamic cycles, the Brayton cycle and the Rankine cycle, and the concept of a combined cycle in Chapter 2. The effect of working fluids to gas and steam turbine cycles is briefly studied in Chapter 3 and carbon capture methods are then introduced in Chapter 4. In Chapter 5 the simulation software Aspen Plus is briefly introduced while in Chapter 6 the process description and process specifications are presented and the two cases that were simulated are explained in more detail. The results of the simulation are displayed and discussed in Chapter 7. Chapter 8 then includes conclusion of the contents of this thesis.

2. GAS AND STEAM TURBINE CYCLES FOR POWER GENERATION

Gas and steam turbine cycles are thermodynamic processes used for power generation. Both processes are essentially based on converting heat energy into mechanical energy. The heat energy needed for the process is usually achieved by combustion of fuel, either directly or indirectly. [4] The effectiveness of a thermodynamic cycle can be expressed as the thermal efficiency of the process which is the ratio of output energy to input energy. The thermal efficiency is defined as

$$\eta_{th} = \frac{W_{net}}{Q_{in}} \tag{2.1}$$

where Q_{in} [W] is the energy input and output energy W_{net} [W] is

$$W_{net} = W_{produced} - W_{required}. \tag{2.2}$$

The net efficiency of a thermodynamic cycle can be expressed as

$$\eta_{net} = \frac{W_{net} - W_{aux}}{Q_{in}} \tag{2.3}$$

where W_{aux} [W] is the required auxiliary work for the process. The net efficiency is a useful indicator for a process that requires auxiliary work that can be considered as external to the thermodynamic cycle itself.

An ideal thermodynamic process that achieves the highest theoretical thermal efficiency in given conditions is called the Carnot cycle. The Carnot cycle is a reversible process where the heat transfer both from the heat source and into the heat sink is isothermal and both the compression and expansion are isentropic. An actual thermodynamic process can never achieve a thermal efficiency of a Carnot cycle due to the fact that there will always be losses involved within the various processes and components of an actual thermodynamic process. Nevertheless, the Carnot cycle is useful when designing or evaluating real thermodynamic cycles as the Carnot cycle shows the theoretical maximum for the thermal efficiency for an actual thermodynamic cycle in a set of conditions. Figure 1 shows the Carnot cycle as the function of specific entropy and temperature.

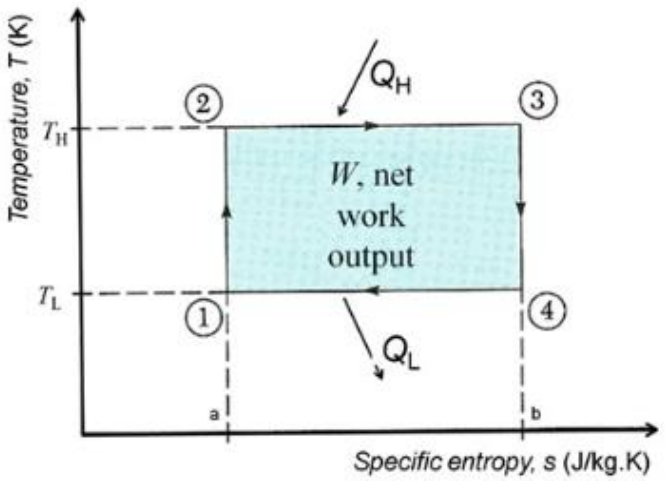

Figure 1. *The Carnot cycle on a temperature-entropy diagram. [5]*

According to the first law of thermodynamics the thermal efficiency of a Carnot cycle is

$$\eta_{th} = \frac{W}{Q_H} = \frac{Q_H - Q_L}{Q_H} \tag{2.4}$$

and then according to the second law of thermodynamics

$$\eta_{th} = \frac{Q_H - Q_L}{Q_H} = \frac{T_H \Delta s - T_L \Delta s}{T_H \Delta s} = \frac{T_H(s_B - s_A) - T_L(s_B - s_A)}{T_H(s_B - s_A)}. \tag{2.5}$$

For the Carnot cycle the thermal efficiency can be expressed as follows

$$\eta_{th} = \frac{T_H - T_L}{T_H} = 1 - \frac{T_L}{T_H} \tag{2.6}$$

where T_H [K] is the temperature at which heat is added to the cycle and T_L [K] is the temperature at which heat is rejected from the cycle and s_B and s_A [J/(kg K)] are the specific entropies. [4] From equation (2.6) it can be seen that for a thermodynamic process resembling the Carnot process the thermal efficiency of the system can be improved by either increasing the heat addition temperature T_H or decreasing the heat rejection temperature T_L. On practical applications the heat rejection temperature usually depends on the atmospheric conditions while the upper limit for the heat addition temperature mainly depends on the material properties of the process components.

One of the differences between gas and steam turbine cycles is that in a gas turbine cycle a major fraction of the gas turbine work output is needed for operating the compressor. In a steam turbine cycle the corresponding unit process only requires a minor fraction of the steam turbine work output. In a steam turbine cycle water is pressurized in liquid form which requires less work than the compression of gases in a gas turbine cycle. On the other hand, the heat addition process for the steam turbine cycle (boiler) requires more

complicated equipment and optimization than the heat addition process for the gas turbine cycle (combustor). [6] The fact that the temperature of the gas turbine exhaust gases is high and at a suitable temperature range that is needed for heat addition in the steam turbine cycle makes the combination of these two thermodynamic cycles very attractive.

Both the gas turbine cycle and the steam turbine cycle are being commonly used around the world as individual simple cycles for power generation but also as parts of combined cycle processes. A combined cycle is a combination of two or more thermodynamic cycles for which many combinations exist and are in use. Perhaps the most generally used combined cycle is a combination of a gas turbine cycle and a steam turbine cycle where the gas turbine cycle is used as the topping cycle and the steam turbine cycle as the bottoming cycle. [7]

2.1 Gas turbine cycle

A simple gas turbine cycle is an open thermodynamic cycle which consists of three stages: compression, combustion and expansion. In an open thermodynamic cycle matter flows in and out of the system. Atmospheric air is brought into the system in the first stage of a simple gas turbine cycle when it is led into the compressor where both pressure and temperature of the working fluid are increased. In the second stage energy is brought to the system as fuel is burned with the compressed air in a combustor or a burner at a constant pressure. In the third stage the hot combustion gases are expanded in the gas turbine. The expansion of the hot combustion gases in the turbine provide mechanical energy which can be used to generate electricity through a generator but also to power the compressor in the first stage. In a simple gas turbine cycle the combustion products are directed into the atmosphere after the expansion. [5] A simple gas turbine cycle is illustrated in Figure 2.

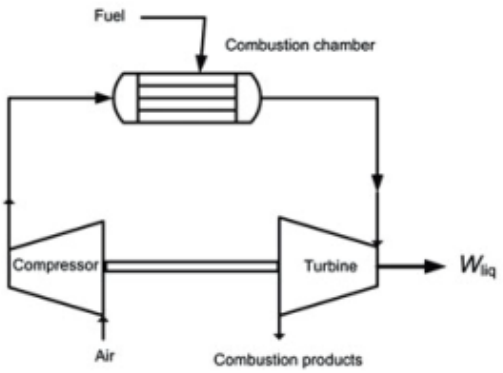

Figure 2. *A simple gas turbine cycle. [5]*

Figure 3 illustrates a single-shaft gas turbine that is assembled in a similar way that was shown in Figure 2 for a simple gas turbine cycle.

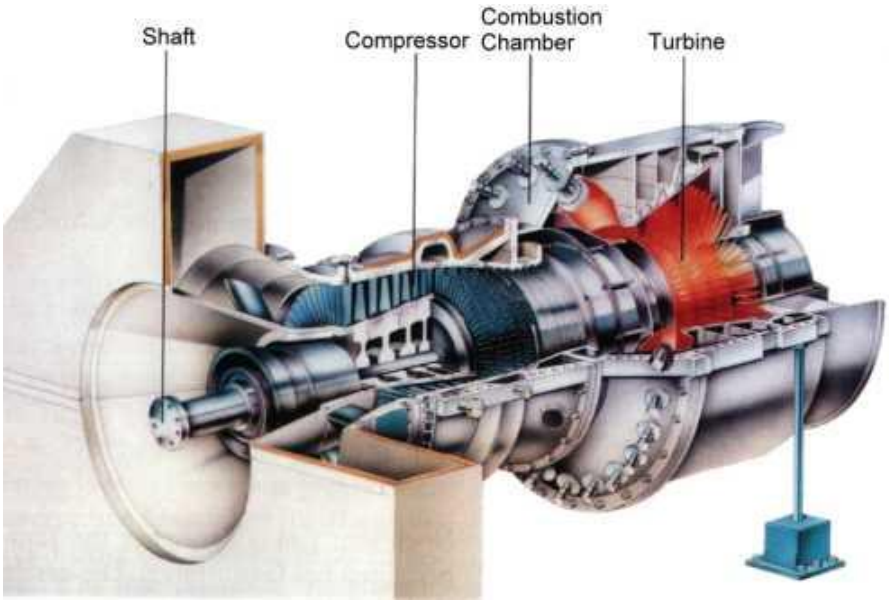

Figure 3. *An illustration of a single-shaft gas turbine. [8]*

The basic concept for the gas turbine cycle has been in use for decades but it has seen major improvements during recent years and today the thermal efficiency for a simple cycle gas turbine can be as high as 45-50% compared to a thermal efficiency of 15% in the 1950s. [7]

2.1.1 Brayton cycle

The Brayton cycle is the basic gas turbine cycle. An ideal Brayton cycle is a closed loop gas turbine cycle where the working fluid can be assumed to be plain air, and the combustion process is replaced by a heat exchanger. As it is a closed loop system, instead of exhausting the air into the atmosphere after the expansion the working fluid is led into another heat exchanger (heat rejection) before going back to the compressor. [5] Figure 4 illustrates the basic concept of an ideal Brayton cycle.

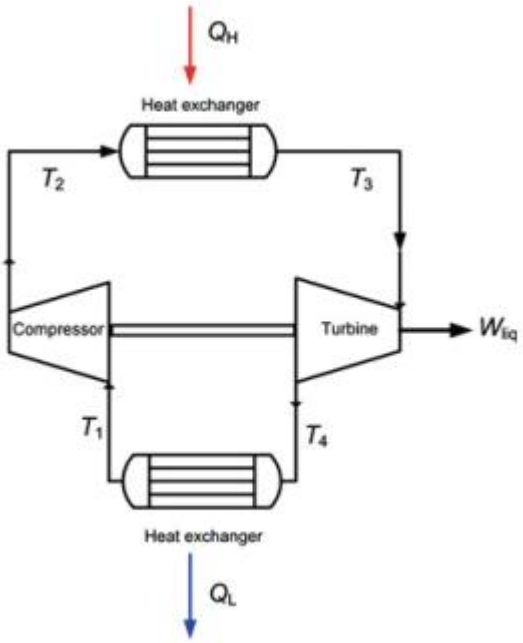

Figure 4. *An ideal Brayton cycle. [5]*

An ideal Brayton cycle consists of four consecutive processes: isentropic compression, isobaric heat addition, isentropic expansion and isobaric heat rejection. These four ideal processes are represented as thermodynamic diagrams in Figure 5. Both diagrams show the heat added (process 2-3), the heat rejected (process 4-1) and the net work (the enclosed area). According to the First Law of Thermodynamics for such a closed loop system the work $W = Q_H - Q_L$ so the thermal efficiency for an ideal Brayton cycle can be defined as a modification of equation (2.1)

$$\eta_{th} = 1 - \frac{Q_L}{Q_H} \tag{2.7}$$

where Q_L [W] is the heat rejected form the system and Q_H [W] is the heat added to the system. From equation (2.7) it can be seen that to increase the thermal efficiency of an ideal Brayton cycle it would require increasing the heat added or decreasing the heat rejected. Analyzing the thermodynamic diagrams in Figure 5 indicates that the heat added and rejected from the system depends on the ratio between maximum and minimum temperature and pressure ratio. Increasing the maximum temperature T_3 or pressure p_2 would increase the heat added to the process while decreasing the minimum temperature T_1 or pressure p_1 would decrease the heat rejected from the process.

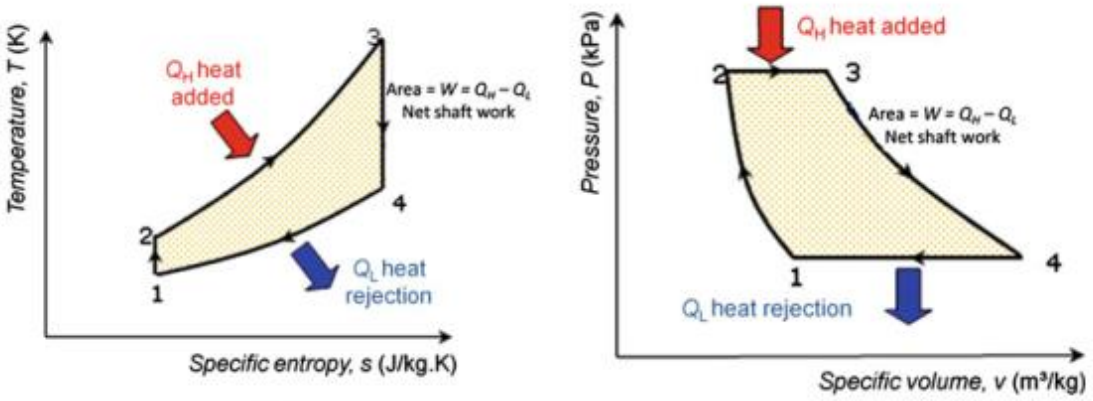

Figure 5. *Temperature-entropy diagram (left) and pressure-volume diagram (right) for an ideal Brayton cycle. [5]*

An actual Brayton cycle differs from an ideal one as there are always losses involved in the different processes of the cycle. The net work produced in a Brayton cycle heavily depends on the compressor: depending on the operating conditions and efficiency of both the compressor and turbine a significant part of the work produced in the turbine might be needed just to operate the compressor. The efficiency of a compressor can be defined as the compressor isentropic efficiency, which is the ratio of isentropic compression work to actual compression work [5]

$$\eta_{sc} = \frac{h_{2s} - h_1}{h_2 - h_1} \tag{2.8}$$

where h is the specific enthalpy [J/kg]. The compression efficiency η_c of a compressor is the isentropic efficiency of a differential compression process. For non-ideal compression the compressor outlet temperature can be calculated with the compression efficiency as follows [9]

$$T_2 = T_1 \left(\frac{p_2}{p_1}\right)^{\frac{1}{\eta_c} * \frac{\kappa - 1}{\kappa}} \tag{2.9}$$

where T_1 [K] is the compressor inlet temperature, p_2 [bar] and p_1 [bar] the compressor outlet and inlet pressures respectively and κ is the ratio of specific heats of the gas in the average temperature $T = \frac{1}{2}(T_1 + T_2)$. The ratio of specific heats is defined as

$$\kappa = \frac{c_p}{c_v} \tag{2.10}$$

where c_p is the specific heat capacity in constant pressure [J/kgK] and c_v is the specific heat capacity [J/kgK] in constant volume. The turbine isentropic efficiency is defined in

a similar way as with the compressor and it is the ratio of actual turbine work to isentropic turbine work [5]

$$\eta_{st} = \frac{h_3 - h_4}{h_3 - h_{4s}}. \tag{2.11}$$

The expansion efficiency η_t of a turbine is the isentropic efficiency of a differential expansion process. For non-ideal expansion the outlet temperature can be calculated with the expansion efficiency as follows [9]

$$T_4 = T_3 \left(\frac{p_3}{p_4}\right)^{-\eta_t * \frac{(\kappa-1)}{\kappa}} \tag{2.12}$$

where T_3 [K] is the turbine inlet temperature, p_3 [bar] and p_4 [bar] the turbine inlet and outlet pressures respectively and κ is the ratio of specific heats of the gas in the average temperature $T = \frac{1}{2}(T_3 + T_4)$. A common parameter used with turbines is also the pressure ratio. The pressure ratio for a turbine is

$$\Pi = \frac{p_3}{p_4} \tag{2.13}$$

where p_3 is the working fluid pressure before the turbine and p_4 is the working fluid pressure after the turbine.

Figure 6 illustrates the differences between isentropic compression (process 1-2s) and actual compression (process 1-2) as well as isentropic expansion (process 3-4s) and actual expansion (process 3-4).

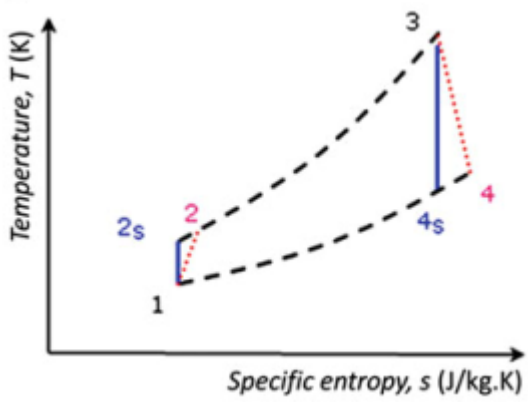

Figure 6. *Actual and isentropic compression and actual and isentropic expansion for a Brayton cycle. [5]*

Figure 7 shows an example of the overall effect of non-ideal compression and non-ideal expansion on the thermal efficiency and on the net work. It illustrates a situation where the expansion efficiency is 0.85 and the compression efficiency is 0.8 and the maximum and minimum temperatures for the process are T_3 = 1200 K and T_1 = 300 K, respectively.

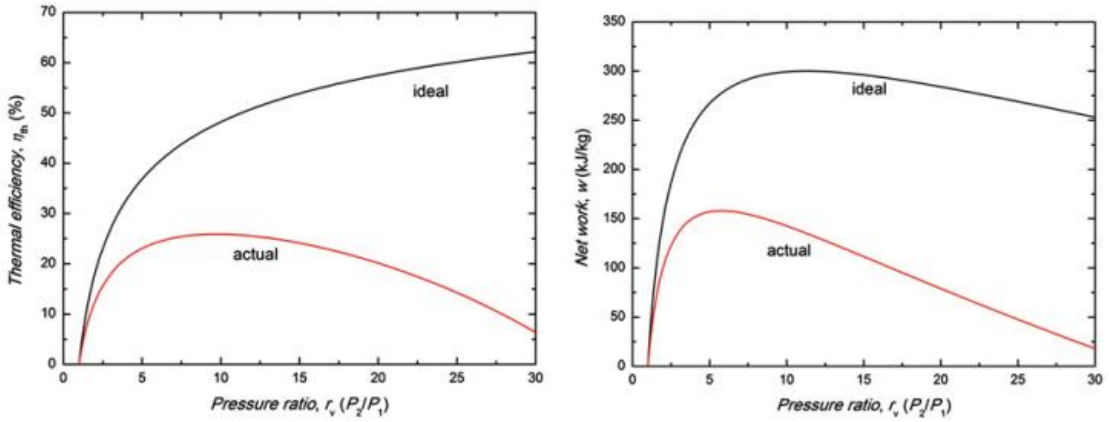

Figure 7. *Actual and ideal thermal efficiency (left) and actual and ideal net work (right) for a Brayton process when η_t = 0.85, η_c = 0.8, T_3 = 1200 K and T_1 = 300 K. Adapted from [5].*

From Figure 7 it is obvious that the isentropic efficiencies of both the compressor and the turbine have major effects on the overall efficiency of the cycle.

2.1.2 Unit processes

A simple gas turbine cycle consists of three major components: a compressor, a combustor and a turbine. The function of the turbine is to decrease the pressure of the working fluid whereas for the compressor the function is to increase the pressure of the working fluid. The function of the combustor is to convert the chemical energy of the fuel to heat energy by combusting it with compressed air. This heat energy then will be converted in the turbine to mechanical energy to power the compressor and to generate electricity through a generator. [4]

The compressor is an essential part of a gas turbine cycle and it has substantial effect on the overall efficiency of the cycle as it uses a major fraction of the power generated by the turbine, from 55-65% [10] to 65-75% [4]. In the compressor atmospheric air is compressed before leading it into the combustor for combustion process. Intercooling can be used in the middle of a multi-stage compression to decrease the work of compression.

There are various types of compressors in use for different kinds of cycles and conditions. Large units (3MW or more) typically use axial compressors while smaller units usually use centrifugal compressors. [4] Centrifugal compressors have a relatively high tolerance for process fluctuations and they are more reliable in use than other kinds of compressors. [10] In centrifugal compressor the fluid, usually air, enters the compressor at the center of a rotating bladed impeller. The rotation imparts a centrifugal force on the air which causes the air to flow radially outward into a stationary diffuser at a very high speed. The velocity of the air is then converted into pressure in both the impeller stage and the stationary diffuser stage. [4, 10]

In axial flow compressors on the other hand the fluid flow into the compressor is parallel with the axis of rotation. An axial compressor is comprised of many stages, all of them including two parts: an impeller followed by a stationary diffusor. In each of these stages the velocity of the fluid is increased first in the impeller part and then this increased velocity is converted into increased pressure for the fluid flow in the stationary part. In an axial compressor the fluid flow goes through all the stages gaining small pressure increases in each stage. By using multiple stages, it is possible to achieve pressure ratios of 30:1 for industrial applications. [10]

The turbine is obviously the main part of a gas turbine cycle. Different types of turbines include radial and axial turbines, the latter being the more used for industrial applications. Radial turbine is largely similar to centrifugal compressor with opposite rotation and reversed flow. Radial turbine has a few advantages over the axial turbine: it costs a lot less than axial turbine and the fact that the work produced in a single stage in the turbine is equivalent to the work needed in two or more stages in the compressor stage. Radial turbine has a lower turbine efficiency compared to axial turbine though so it depends on the situation which kind of turbine suits best for the set of conditions. [10] Axial turbine also has similarities with its corresponding compressor, axial flow compressor, and the fluid flow enters and exits the turbine parallel with the axis of rotation. An axial turbine usually has more than one stage with every stage consisting of a stationary nozzle followed by rotating impeller. There are two types of stages in axial turbines: so called reaction type and impulse type. [10] The reaction type means that the enthalpy drop happens in both in the nozzle and in the impeller, and the degree of reaction can be defined as the ratio of change in the impeller to the change in total enthalpy [9]

$$r = \frac{\Delta h_s''}{\Delta h_s' + \Delta h_s''} \tag{2.14}$$

where $\Delta h_s''$ [J/kg] is the enthalpy change in the impeller section and $\Delta h_s'$ [J/kg] is the enthalpy change in the nozzle section. Figure 8 illustrates the enthalpy change in the impeller and nozzle sections of the turbine.

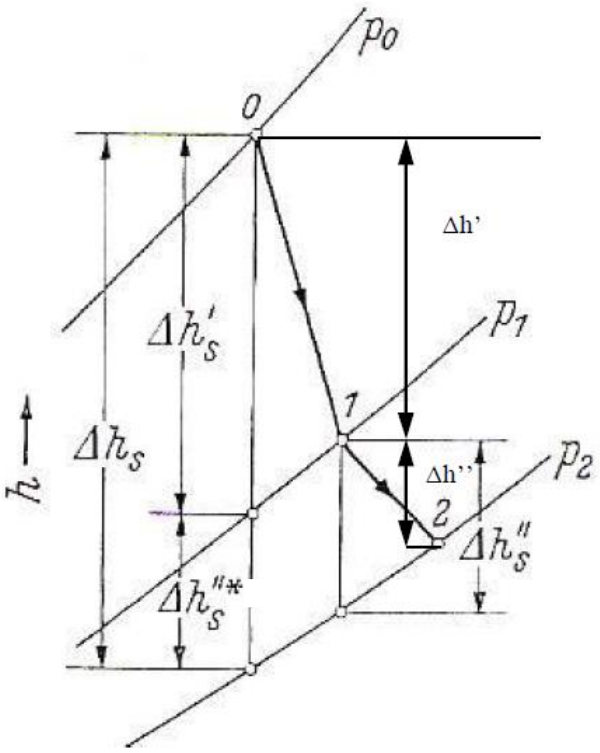

Figure 8. *Enthalpy changes in the impeller and nozzle sections of a turbine. The actual enthalpy changes are marked with Δh' and Δh'' for nozzle section and impeller section, respectively. Isentropic enthalpy changes are marked with the subscript 's'. [9]*

The combustor is where heat is added into the gas turbine cycle. In the combustor fuel is burned with compressed air from the compressor. The high pressure, high temperature combustion gases are then led to the turbine to complete the gas turbine cycle. Different kinds of combustors exist and are in use but the three main types are annular, tubular and tubo-annular combustors. Three zones featured in all types of combustors are: a recirculation zone where fuel is partly burned and evaporated to prepare it for swift combustion in the following zones, a burning zone where all of the fuel will be burned in an ideal situation, and a dilution zone where the hot combustion gases will be mixed before entering the gas turbine. The efficiency of a combustor can be estimated by the completeness of the combustion process which is the ratio of actual enthalpy increase to the theoretical enthalpy increase during the combustion process. [10]

$$\eta_{combustor} = \frac{\Delta h_{actual}}{\Delta h_{theoretical}} \tag{2.15}$$

where Δh [J/kg] is the enthalpy change. The theoretical enthalpy increase represents the heating value of the fuel in use.

2.1.3 Methods for improving efficiency

For an open loop gas turbine cycle a number of ways can be used to improve the cycle efficiency including heat regeneration and intercooling. An open loop gas turbine cycle with heat regeneration is illustrated in Figure 2. As can be seen in Figure 2, the combustion gases are being directed to the atmosphere after expansion and at that point the gases are at a relatively high temperature which usually also happens to be higher than the temperature of the compressed air entering the combustor. It is quite obvious that the excess heat of the combustion gases could be used in a recuperative way earlier in the process. A counter-flow heat exchanger could be installed before the combustor where the combustion gases would be used to heat the compressed air. The added heat before the combustor would lead to fuel saving. [5] Figure 9 illustrates a modified open loop gas turbine cycle with heat regeneration.

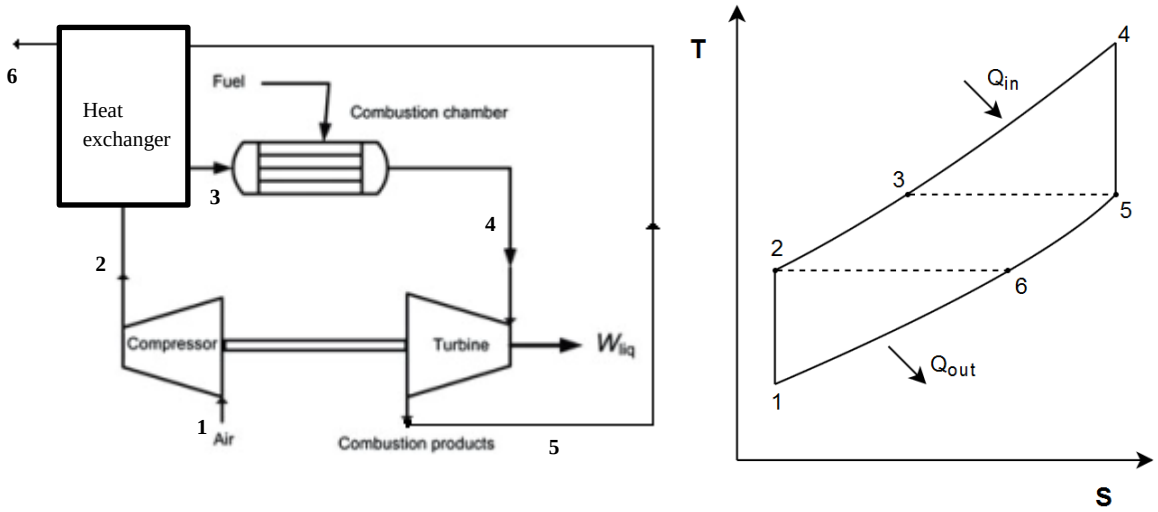

Figure 9. *A simple open loop gas turbine cycle with heat regeneration (left), adapted from [5]. Heat regeneration on a temperature-entropy diagram (right).*

Another way of improving the efficiency of an open loop gas turbine cycle is to use so called intercooling in the compression section of the gas turbine cycle. The temperature of the fluid flow increases as it is compressed and this increase in temperature leads to higher volume for the fluid. Intercooling is a method where the compression is done in two parts and the fluid flow is cooled between these two parts. After the first compression part the fluid is at a state of higher pressure and temperature compared to the state of the fluid before the compressor. By cooling the fluid after the first part of compression the temperature of the fluid decreases and as a consequence the volume of the fluid also decreases leading to less compression work needed in the second part of compression. As the compressor uses a major fraction of the turbine work output, this deduction in the amount of work needed to operate the compressor directly leads to higher net work output

form the gas turbine cycle. [11] On the other hand, intercooling increases the fuel need. The compressed fluid is heated in the combustor to a certain turbine inlet temperature and as a consequence a lower compressor outlet temperature leads to higher amount of heating needed in the combustor. Figure 10 presents intercooling in a Brayton cycle in a temperature-entropy diagram.

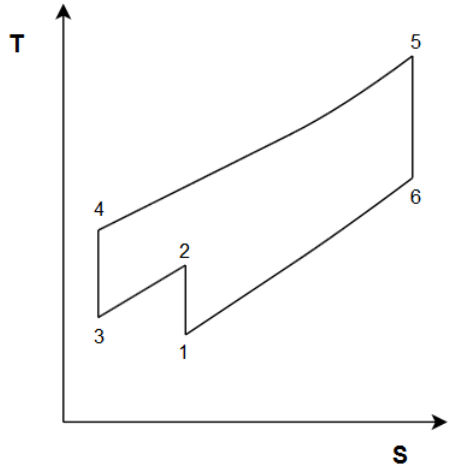

Figure 10. *Intercooling in a Brayton cycle on a temperature-entropy diagram. Sub-processes 1-2 and 3-4 express compression and sub-process 2-3 expresses intercooling.*

Water injection is another way of implementing intercooling in which water is injected into the gases before or during compression. The water injected will vaporize which will decrease the gas temperature. The injected water will increase the mass flow of the process leading to higher work output from the gas turbine. [9] While intercooling is a method where the net work output is increased by decreasing the work needed for compression, reheating is a method where net work output is increased by increasing the turbine work output. Reheating is a method where the expansion is divided into two or more stages and the working fluid is reheated in between the stages. Figure 11 illustrates the reheating process. [10]

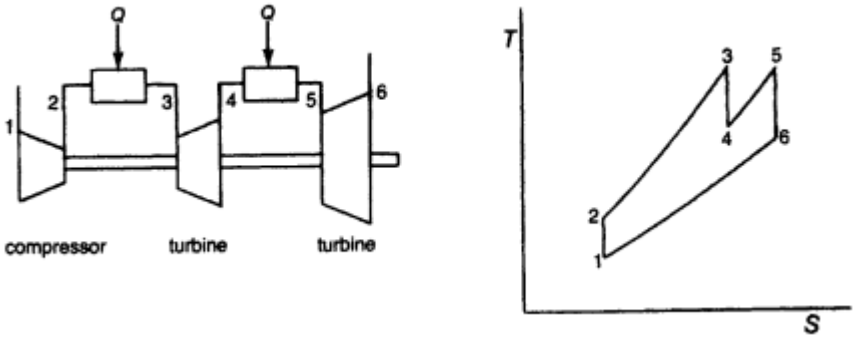

Figure 11. *A schematic (left) and a temperature-entropy diagram (right) of reheating. Adapted from [10].*

The Ericsson cycle is a theoretical thermodynamic cycle that is a modification of the Brayton cycle with better thermal efficiency. First of all, the compression and expansion in Ericsson cycle happen at the same time which is unique and both of the unit processes are isothermal instead of isentropic as in ideal Brayton cycle. The Ericsson cycle also includes heat regeneration where the rejection heat is used in the isobaric heat addition process. The thermal efficiency of the Ericsson cycle is the same as in Carnot cycle. When using both reheating and intercooling it is possible for a cycle to get closer to the Ericsson cycle by having the number of stages used in intercooling and reheating approach infinity and thus to get closer to the theoretical maximum thermal efficiency. [6]

The gas turbine inlet temperature is limited by the turbine blade material properties. [4] New materials that can withstand higher temperatures and more effective turbine blade cooling techniques will allow for the use of higher turbine inlet temperatures in near future and thus leading to higher efficiency for the gas turbine cycle.

2.2 Steam turbine cycle

A steam turbine cycle is a closed loop thermodynamic process that is used for power generation all over the world, and it is in fact the most used thermodynamic cycle used for electricity generation [7]. It is based on phase change for the working fluid which in most applications is water. A basic steam turbine cycle consists of four unit processes: a boiler, a steam turbine, a condenser and a pump. A basic steam turbine cycle is illustrated in Figure 12. The working fluid (liquid) is compressed to high pressure by the pump before entering the boiler. In Figure 12 the boiler is illustrated having three different sections where the working fluid (liquid) is first heated to saturated liquid in section 2a (also called the economizer), evaporated to steam in section 2b (also called the evaporator) and then heated to superheated steam in section 3 (also called the superheater). The high pressure, high temperature steam is then expanded in the turbine generating electricity and finally the expanded steam is condensed back to liquid form in

the condenser. [7] Heat is added into the system in the boiler part of the cycle and heat is rejected from the cycle in the condenser part. The steam turbine on the other hand generates power while the pump requires power for pressurizing the working fluid. In practice the heat addition in the boiler section can be achieved by burning fuel or alternatively a heat exchanger can be applied instead of the boiler if a sufficient heat source is available.

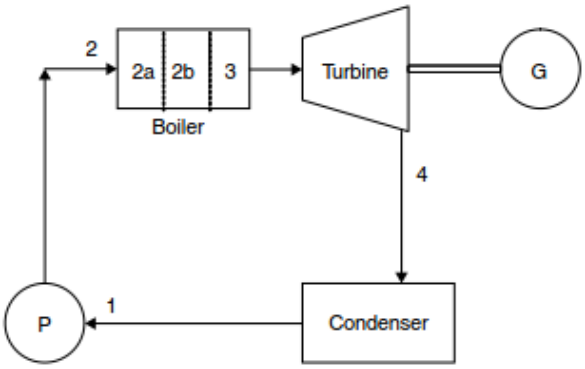

Figure 12. *A basic steam turbine cycle. [7]*

2.2.1 Rankine cycle

An ideal Rankine cycle is basically similar to that of Figure 12 and it is illustrated as a temperature-entropy diagram in Figure 13. First, water enters the pump where it undergoes isentropic pressurization to the desired pressure before entering the boiler. In the boiler water is heated to saturation temperature, evaporated to steam and superheated. The superheated steam then enters the steam turbine where it undergoes isentropic expansion. After the turbine the expanded steam enters the condenser where heat is rejected to cold water. In the condenser the steam condenses to saturated liquid in an isobaric process and is then lead back to the pump for repeating the cycle. [7]

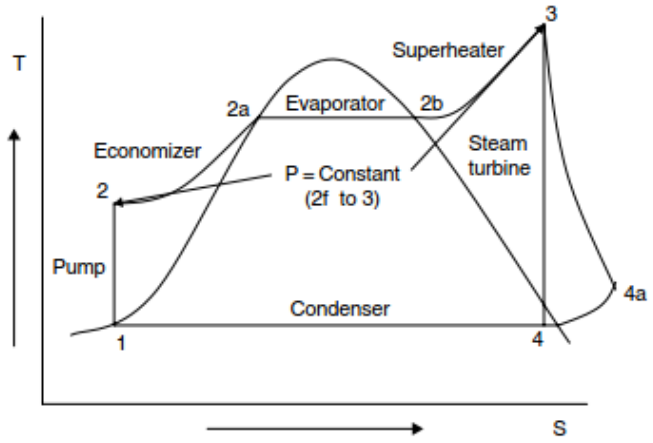

Figure 13. *A temperature-entropy diagram of a Rankine cycle. The temperature increase in the sub-process 1-2 is overemphasized for illustration purposes. [7]*

In Figure 13 the process 3-4 represents ideal (isentropic) expansion and process 3-4a represents the real expansion process. The temperature increase in Figure 13 is overemphasized for the sub-process 1-2 which represents the pressurization of liquid water in the pump.

2.2.2 Unit processes

A basic steam turbine cycle consists of four components: a boiler, a turbine, a condenser and a pump. The boiler is where the working fluid (water) is transformed into steam. The working fluid flows through the boiler inside several pipes and it is designed so that the heat exchange area of the pipes is sufficient to enable the phase change and desired steam parameters (superheated steam) for the working fluid at the boiler outlet. A heat exchanger can also act as the boiler in a steam turbine process if sufficient heat is available from an outside source. [5]

Due to three distinctive processes occurring in the boiler, it may be considered as having three functional sections that are the economizer, the evaporator and the superheater. In order to maximize the thermal efficiency of the boiler, especially in a large system, many stages of each of these three sections may be used. The economizer is the part where the working fluid flows into first when entering the boiler after being pressurized in the pump. The economizer is used to heat the working fluid to near the boiling point by using heat from the combustion gases near the boiler outlet and is essential for maximizing the boiler efficiency. The evaporator is the second section of the boiler and it is where the working fluid undergoes the phase change from liquid to steam at a constant temperature. The last section of the boiler is the superheater where the temperature of the steam is increased above the saturation temperature further increasing the specific enthalpy of the steam. [4]

The boiler should be optimized in a way that the water is heated as close to boiling point as possible in the economizer section and that all the water is turned into steam completely in the evaporator section. The superheater section then is where the steam will be heated to the desired final state before entering the steam turbine.

In a steam turbine cycle the turbine is arguably the main component as it is where the energy of the working fluid can be converted into mechanical energy and then into electricity. The enthalpy of the working fluid is a function of temperature and pressure and inside the turbine a part of the enthalpy will be converted in to kinetic energy which is used to rotate a generator to generate electricity. At the turbine outlet the steam is at a state of lower temperature and lower pressure and consequently has lower enthalpy compared to the steam conditions at the turbine inlet. [5]

The condenser is a heat exchanger where the steam from the turbine is condensed to saturated liquid by rejecting heat to a stream of cold water. Typically, the cold water and the condensing steam are separated by metallic surface in a shell-and-tube or a tube-in-tube configuration where the steam condensates on the surfaces cooled by the cold water stream. The condensed steam then falls to the bottom of the condenser from where it can be extracted. The cold water stream used in the condenser can be obtained from nearby rivers, lakes or sea or then a cooling tower can be used if no nearby water source is available. [5]

The pump is used to pressurize the working fluid to the pressure level of the boiler which is the same high pressure that is needed for the expansion process. The pump work is

$$P_p = \dot{m}(h_1 - h_2) \tag{2.16}$$

where $\dot{m}$ [kg/s] is the mass flow through the pump, h_1 [kJ/kg] and h_2 [kJ/kg] are the specific enthalpies of the working fluid before and after the pump, respectively. As water is practically non-compressible, the pump work can be expressed as

$$P_p = \dot{m} v \Delta p \tag{2.17}$$

where v [m^3/kg] is the specific volume of water and Δp [Pa] is the pressure difference over the pump.

2.2.3 Methods for improving efficiency

The steam turbine cycle efficiency can be improved by using various methods which include superheating, increasing the turbine inlet pressure, lowering the turbine outlet pressure and steam reheating. [12] Usually a combination of these methods can be used to achieve optimal and desired outputs for certain operating conditions and parameters.

Superheating means that the steam is heated above the saturation temperature. Figure 14 illustrates the effect of different degrees of superheating and it can be seen that for a certain inlet pressure a higher inlet temperature leads to better thermal efficiency. From the temperature-entropy diagram on Figure 14 it can also be seen that a higher degree of superheating leads to less moist steam. Typical turbine inlet temperatures are in the range 540-560 ºC because of material limitations [12] but inlet temperatures of around 600 ºC are also currently used for supercritical steam turbines. [13,14] Further development in material technology might make it possible to use even higher temperatures. [12]

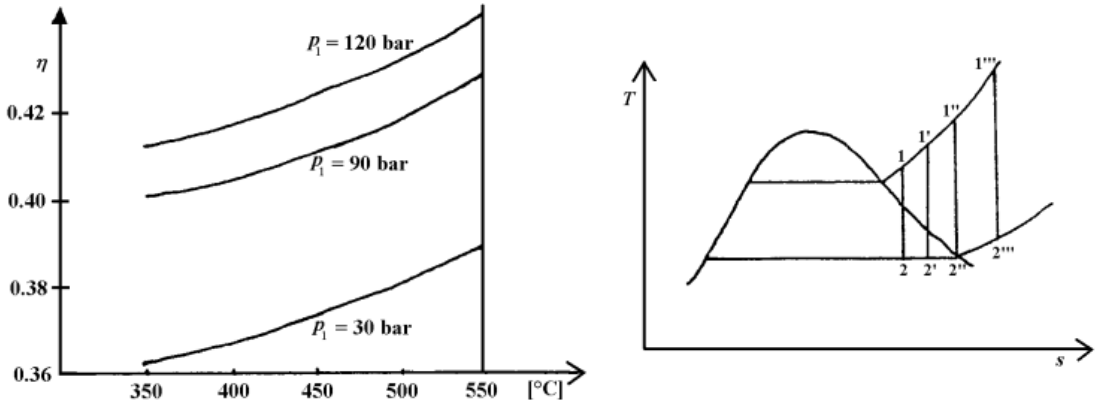

Figure 14. *Thermal efficiency of a Rankine cycle as a function of inlet temperature, when condenser pressure is p_2 = 0.04 bar (left) and the effect of superheating on a temperature-entropy diagram (right). Adapted from [12].*

By increasing the turbine inlet pressure the thermal efficiency of the steam turbine cycle is increased as the average heat addition temperature gets higher. On the other hand, higher pressure leads to higher costs due to material requirements. Figure 15 illustrates the effect of increasing turbine inlet pressure on a temperature-entropy diagram and also the dependency of thermal efficiency on the turbine inlet pressure for a certain temperature. From Figure 15 it can also be seen that higher turbine inlet pressure leads to more moisture on the turbine outlet steam which then limits the turbine inlet pressure because of not too much moisture can be allowed in the turbine to avoid erosion caused by the moisture. [12]

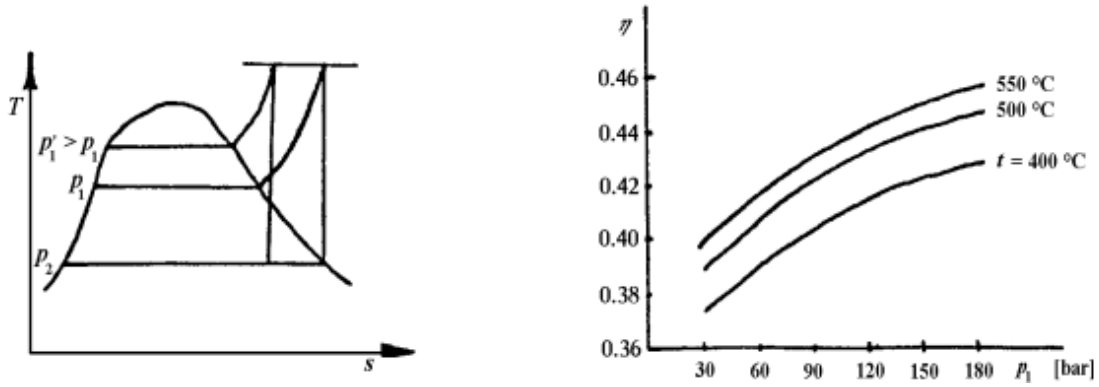

Figure 15. *The effect of increasing the turbine inlet pressure on a Rankine cycle on a temperature-entropy diagram (left) and the thermal efficiency as a function of turbine inlet pressure when turbine outlet pressure is p_2 = 0.4 bar (right). Adapted from [12].*

Lowering the turbine outlet pressure will increase the thermal efficiency as can be seen from the left side of Figure 16. On the other hand, as the turbine outlet pressure gets lower, the specific volume of steam increases which leads to larger size of the turbine and consequently to higher costs. Also the moisture level of the steam increases when the turbine outlet pressure gets lower. The turbine outlet pressure is determined by the condensation temperature in the condenser. [12] In this regard the Nordic countries have an advantage over some warmer countries as lower temperatures for the cold water used in the condenser allow the use of lower condensation pressure.

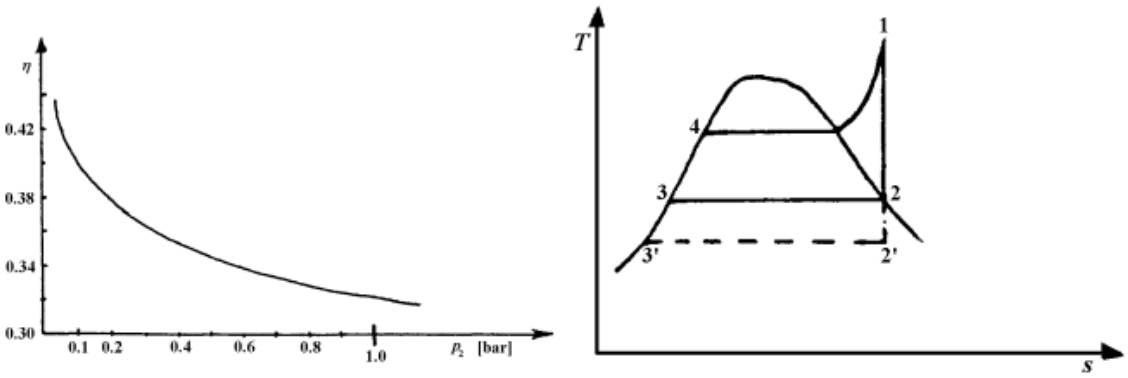

Figure 16. *The thermal efficiency as a function of turbine outlet pressure (left) and the effect of lowering the turbine outlet pressure on a temperature-entropy diagram (right) on a Rankine cycle. Adapted from [12].*

Steam reheating is a method in which the expansion in the steam turbine section is done in stages and the steam is reheated between these stages. After each expansion stage the steam is reheated in the superheater section of the boiler before entering the next expansion stage as a superheated steam. Usually two or three stages are used in steam reheating processes. Figure 17 illustrates the steam reheating method.

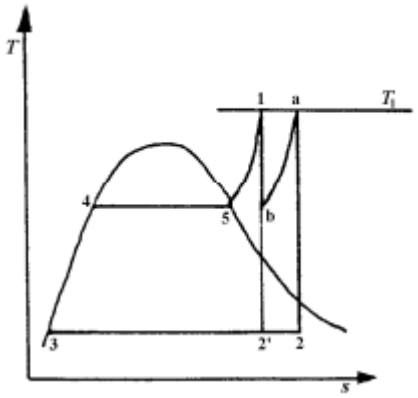

Figure 17. *The effect of steam reheating on a Rankine cycle on a temperature-entropy diagram.[12]*

2.3 Combined cycle

A combined cycle is a combination of two or more thermodynamic cycles. The most common combined cycle is the combination of a gas turbine cycle and a steam turbine cycle which can sometimes be called the Brayton-Rankine cycle. [7] The Carnot efficiency for an individual gas turbine cycle or a steam turbine cycle is around 45-57% but for a combined cycle it can be even 65-78% so it is quite obvious that a combined cycle system is attractive, even though the differences for the actual thermal efficiencies are slightly smaller. [15]

In a basic combined cycle energy is brought into the system only in the topping cycle. For a basic combined cycle, the electrical efficiency is then

$$\eta_{elec} = \frac{P_{GT}+P_{ST}}{Q_{GT}} \tag{2.18}$$

where P_{GT} is the gas turbine net power output, P_{ST} is the steam turbine net power output and Q_{GT} is the combustor fuel consumption in the topping cycle.

2.3.1 Configuration

The schematic for a basic combined cycle is shown in Figure 18. In a typical combined cycle, the gas turbine cycle works as the topping cycle and the steam turbine cycle works as the bottoming cycle. [7] For such a combination many variations exist and there can be a couple of gas turbines operating with one steam turbine or then one gas turbine might be operated with one steam turbine. Also each turbine might have their own generator or then the turbines might be operated on a single shaft as illustrated by Figure 18. [11]

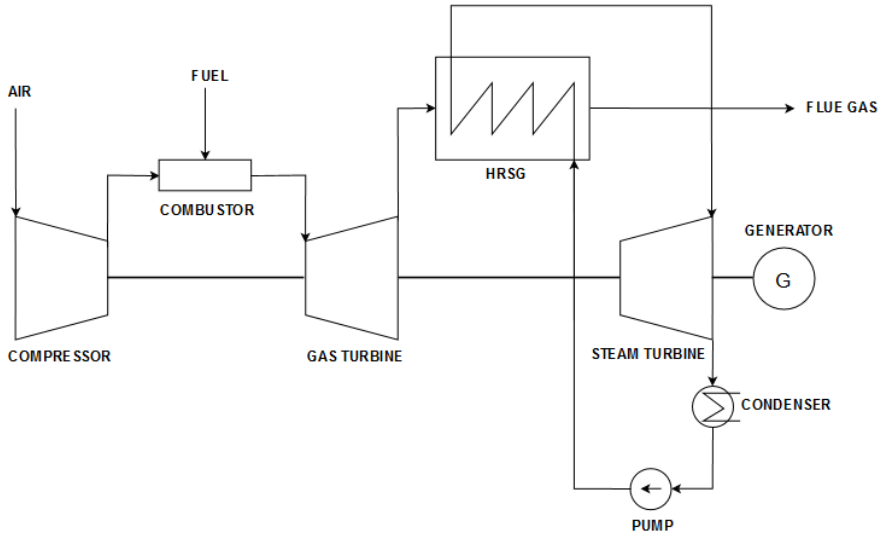

Figure 18. *The schematic of a basic combined cycle.*

In a combined cycle the individual cycles are connected with a heat recovery steam generator (HRSG). The HRSG connects the two cycles while it also substitutes the boiler in the steam turbine cycle. The HRSG uses heat from the high temperature exhaust gases of the gas turbine cycle to produce steam in the bottoming cycle.

2.3.2 Unit processes

For a combined cycle the main operational principles of the individual cycles are the same as when they are operated on their own as simple cycles. The main difference here is the HRSG which is vital for the efficient use of the combined cycle system. [7] Different types of heat exchangers are in use with the common function of transferring heat from a high-temperature fluid to a low-temperature fluid. The heat exchanger types in use include shell-and-tube heat exchangers, concentric tube heat exchangers, plate-and-frame liquid/liquid heat exchangers and finned-tube heat exchangers, for example. An HRSG

can be characterized as direct-contact or indirect-contact and the different flow arrangements include counterflow, parallel flow, crossflow and mixed flow. Counterflow is arguably the most efficient flow arrangement for a HRSG as it allows for the greatest temperature difference while requiring the least heating surface. The rate of heat transfer between the high-temperature fluid and the low-temperature fluid depends on the logarithmic temperature difference between the fluids. [4] The logarithmic temperature difference is defined as

$$\Delta T_{LMTD} = \frac{\Delta T_A - \Delta T_B}{\ln(\frac{\Delta T_A}{\Delta T_B})} \tag{2.19}$$

where ΔT_A is the temperature difference between the high-temperature fluid and the low-temperature fluid at end *A* and ΔT_B is the temperature difference between the high-temperature fluid and the low-temperature fluid at end *B*.

In a reversible heat transfer process the heat transfer is isothermal, such as in the ideal Carnot cycle. The change in entropy in an isothermal heat transfer process is

$$\Delta S = \frac{Q_{rev}}{T} \tag{2.20}$$

where Q_{rev} [W] is the heat transferred reversibly to the system and T [K] is the absolute temperature in which heat is transferred. In practice the heat transfer is never reversible. The entropy change is greater in an irreversible heat transfer process than in a reversible heat transfer process. The relative irreversibility of a heat transfer process can be expressed as

$$\frac{\Delta S}{S} \approx \frac{\Delta T}{T} \tag{2.21}$$

where ΔS [J/K] is the difference between the entropy changes of the irreversible and reversible processes, ΔT [K] is the average temperature difference between the two heat sources and T [K] is the average temperature at the heat transfer interface. From equation (2.21) it can be seen that the smaller the temperature difference between the hot and cold streams in a counterflow heat exchanger are, the lower the irreversibility of the heat transfer process.

Figure 19 illustrates the temperature-entropy diagram of a combined cycle process where Brayton cycle is used as the topping cycle and Rankine cycle is used as the bottoming cycle.

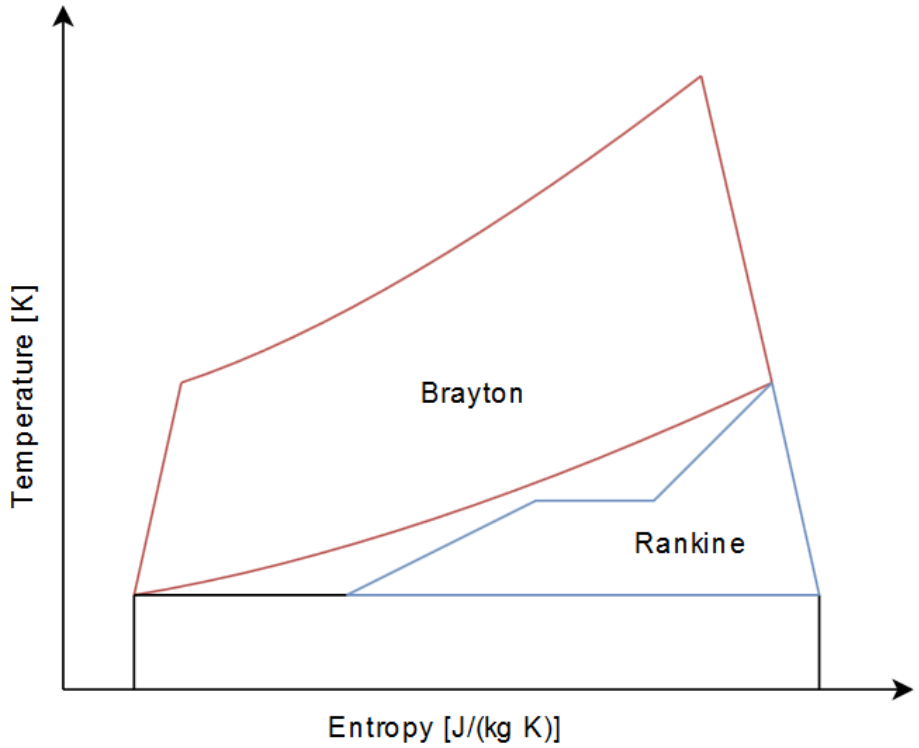

Figure 19. *The temperature-entropy diagram of a combined cycle process where Brayton cycle is used as the topping cycle and Rankine cycle is used as the bottoming cycle.*

In Figure 19 the area between the Brayton and Rankine processes represents the energy loss from the Brayton cycle. From Figure 19 it can be seen that the smaller the temperature difference between the hot and cold streams in the section of the combined cycle where heat is transferred from Brayton cycle to Rankine cycle, the smaller the area is in the figure and thus the smaller the irreversibility of the heat transfer process.

2.3.3 Methods for improving efficiency

New, innovative ways of implementing the combined cycle concept are likely to make it possible to improve the efficiency of the combined cycle. New configurations of the combined cycle as well as adopting unconventional working fluids for the otherwise relatively conventional combined cycle could make way for efficiency increases in the near future. The advancing material properties and cooling techniques will make it possible to adopt higher temperatures and higher pressures in different sections of the combined cycle. This will make it possible to achieve higher efficiencies considering the unit operations of a combined cycle and therefore better overall efficiency.

In this thesis a novel configuration of the combined cycle is simulated. In addition the use of an unconventional working fluid and its effect to the process overall performance is studied in the simulation.

3. WORKING FLUIDS IN GAS AND STEAM TURBINE CYCLES

The working fluid for a conventional steam turbine cycle consists of water whereas the working fluid for a conventional gas turbine cycle has a major fraction of nitrogen due to using air as the oxidizer in the combustion process. The composition of the working fluid depends on many factors including the fuel chemical composition and the combustion process. In addition to nitrogen, the working fluid for a conventional gas turbine cycle commonly consists of water vapor and carbon dioxide and may contain other gaseous chemical components, such as nitrogen oxides and carbon monoxide. The composition of the working fluid can have a major effect on the process due to the different chemical properties of the different chemical components.

3.1 Gas turbine cycles

Developing new ways of improving the gas turbine cycle is important in order to achieve greater process efficiencies or diminish the emissions associated with the gas turbine cycle. Increasing the process efficiencies and diminishing the emissions both work for the necessary reduction of overall emissions from power generation. Unconventional ways of implementing the gas turbine cycle may include the use of different working fluids. Oxyfuel combustion is one method that can be used for controlling the carbon dioxide emissions of a gas turbine cycle and in which the working fluid consists of mainly carbon dioxide and water. Oxyfuel combustion is presented in more detail in Chapter 4. Oxyfuel combustion was used in the simulation model of the combined cycle simulated in this thesis.

Due to the difference in the composition of the working fluid between an oxyfuel combined cycle and a conventional air-fired combined cycle, the working fluids have distinct thermodynamic properties. Different thermodynamic properties affect the performance of the unit processes in the gas turbine cycle. Thus additional chemical components could be used to balance the overall working fluid thermodynamic properties. Argon was suggested by [16] for more effective use of an oxyfuel combined cycle. In this thesis the addition of argon in the working fluid in the oxyfuel combined cycle is simulated and its effects analysed.

The thermodynamic properties of the working fluid for a gas turbine cycle depend on the thermodynamic properties of each of the chemical components. For an ideal gas the ratio of specific heats is connected with the degrees of freedom of the molecule and can be expressed as

$$\kappa = 1 + \frac{2}{f} \tag{3.1}$$

where f is the degrees of freedom of a molecule. For a molecule it is possible to have three translational degrees of freedom, three rotational degrees of freedom and a number of vibrational degrees of freedom depending on the number of atoms in the molecule. The effect of vibration on heat capacity is generally negligible at room temperatures. At room temperature there are three degrees of freedom for a monatomic ideal gas, while five degrees of freedom for diatomic ideal gas and six degrees of freedom for triatomic ideal gas. Therefore, according to equation (3.1) the ratio of specific heats is 1.67 for a monatomic ideal gas, 1.4 for diatomic ideal gas and 1.33 for triatomic ideal gas. However, for real gases the ratio of specific heats depends on the temperature. For real gases more degrees of freedom become relevant at temperatures higher than the room temperature, leading to decreasing ratio of specific heats.

A conventional combined cycle process uses air as the fuel oxidant. Air consists of roughly 78 vol-% N_2 which is mainly inert during the combustion process. This leads to the combustion gases having a significant component of diatomic nitrogen gas. Using pure oxygen as the oxidant in an oxyfuel combustion process, on the other hand, leads to the working fluid being composed of mainly carbon dioxide and water, both triatomic gases. The difference in the composition of the combustion gases in a conventional combined cycle and in an oxyfuel combined cycle results in relevant difference in the ratio of specific heats of the combustion gases. According to equation (2.12), the lower ratio of specific heats for combustion gases in an oxyfuel combined cycle leads to higher exhaust temperatures after expansion in gas turbine when compared to conventional combined cycle with an equal pressure ratio. From equation (2.12) it can also be seen that in order to reach similar exhaust temperatures with conventional and oxyfuel gas turbine expansion, a lower gas turbine discharge pressure is needed for a fixed gas turbine inlet pressure.

Air consists of approximately 0.9 vol-% of argon which is a monatomic noble gas. A compilation of some physical properties for water, carbon dioxide, nitrogen and argon at chosen states are presented in Table 1. Table 1 presents the ratio of specific heats and the specific heat at constant pressure at the state of 600 ºC, 1 bar and at the state of 1400 ºC, 20 bar which were chosen as the expansion will be simulated later in the thesis at around these two states.

Table 1. *Basic physical properties of water, carbon dioxide, argon and nitrogen. Ratios of specific heat and specific heat at constant pressure for gases from Aspen Plus property analysis using Peng-Robinson equation of state.*

Substance	H_2O	CO_2	Ar	N_2	Unit
Molar mass	18.015	44.010	39.948	28.013	g/mol
Type of molecule	triatomic	triatomic	monatomic	diatomic	-
Ratio of specific heats (κ) at 600 ºC, 1 bar	1.267	1.189	1.668	1.353	-
Ratio of specific heats (κ) at 1400 ºC, 20 bar	1.208	1.163	1.668	1.308	-
Specific heat at constant pressure (c_p) at 600 ºC, 1 bar	39.676	52.393	20.791	31.920	J/(mol K)
Specific heat at constant pressure (c_p) at 1400 ºC, 20 bar	48.883	59.559	20.801	35.308	J/(mol K)

From Table 1 it can be concluded that a mixture of water and carbon dioxide result in a lower ratio of specific heats than a mixture with high concentrations of nitrogen. According to equation (2.12), a lower ratio of specific heats leads to higher exhaust temperatures after expansion in gas turbine when compared to a mixture with higher ratio of specific heats with an equal pressure ratio. From Table 1 it is also clear that the addition of argon to a mixture of water and carbon dioxide will increase the ratio of specific heats of the mixture. From equation (2.12) it can be seen that in order to reach similar exhaust temperatures using mixtures with and without argon, a lower gas turbine discharge pressure is needed with a mixture containing argon for a fixed gas turbine inlet pressure.

Two types of working fluids are used in the simulation of an oxyfuel combined cycle later in this thesis: one consisting of mainly carbon dioxide and water and the other one consisting of mainly carbon dioxide, water and argon. The addition of argon will increase the ratio of specific heats of the mixture and will presumably make two things possible in a gas turbine: to reach lower exhaust temperatures with a certain pressure ratio or to reach a certain exhaust temperature with lower pressure ratio. The behavior of the different working fluids should be evident in the results of the simulation.

Oxyfuel combustion allows for a relatively simple separation of carbon dioxide from the process. But when carbon dioxide is separated from a mixture of carbon dioxide and argon, the separation requires work. The theoretical separation work is the difference between that of a complete separation of the whole mixture and that of the returned mixture without the rejected part of carbon dioxide [16]

$$W_{AR} = \dot{n}_1 R_u T[\, a_1 * \ln(a_1) + b_1 * \ln(b_1)\,] - \dot{n}_2 R_u T[\, a_2 * \ln(a_2) + b_2 * \ln(b_2)\,] \quad (3.2)$$

where R_u = 8.314 J/(mol K) is the gas constant, T [K] is the temperature of the mixture, $\dot{n}$ [kmol/s] is the molar flow of the mixture, a is the molar fraction of argon in the mixture, b is the molar fraction of carbon dioxide in the mixture and the subscript 1 stands for the mixture before the separation and the subscript 2 for the mixture after the separation.

3.2 Steam turbine cycles

Conventional steam turbine cycles use water as the working fluid. Other variations of the steam turbine cycle exist, for example the Organic Rankine Cycle (ORC). An ORC is based on the Rankine cycle in which the working fluid is an organic fluid other than water. Depending on the working fluid, the ORC can be used at temperature levels lower than those required for the water-steam phase change. Some working fluids that have been studied for the use in an ORC include ethanol, benzene and toluene, for example. [17]

Another variation of a conventional steam turbine cycle is a supercritical steam cycle in which the working fluid is also water. In a supercritical steam cycle the working fluid is used in conditions above its critical point. Critical point is a point used in thermodynamics as a point where phase boundaries disappear. When both the temperature and pressure of water exceed the critical point, water becomes supercritical steam. Supercritical is a state of fluid where liquid and gaseous states are indistinguishable.

In the oxyfuel combined cycle process simulated in this thesis, the recirculation water enters the middle section of the heat recovery steam generator (HRSG) at above critical pressure and then goes through the transition from water to supercritical steam after passing the critical temperature. The oxyfuel combined cycle process simulated in this thesis will be presented in more detail in Chapter 6.

A schematic of the liquid-vapor critical point in a pressure-temperature diagram is presented in Figure 20. Water has a critical point at 221.2 bar and 374.15 ºC.

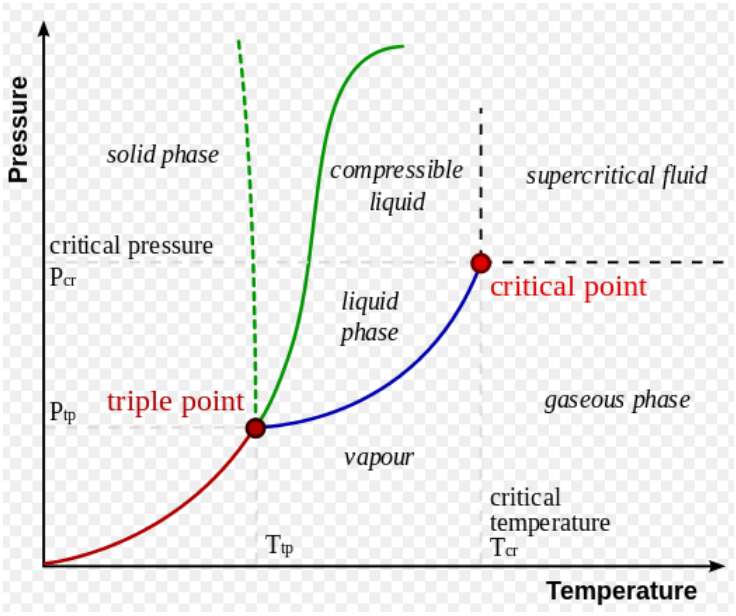

Figure 20. *The liquid-vapor critical point on a pressure-temperature diagram.[18]*

Figure 21 presents the simplified situation in an HRSG where hot combustion gases reject heat to water. Figure 21 illustrates the situation for both the phase change from liquid to steam at subcritical conditions and the transition from liquid to supercritical steam at supercritical conditions.

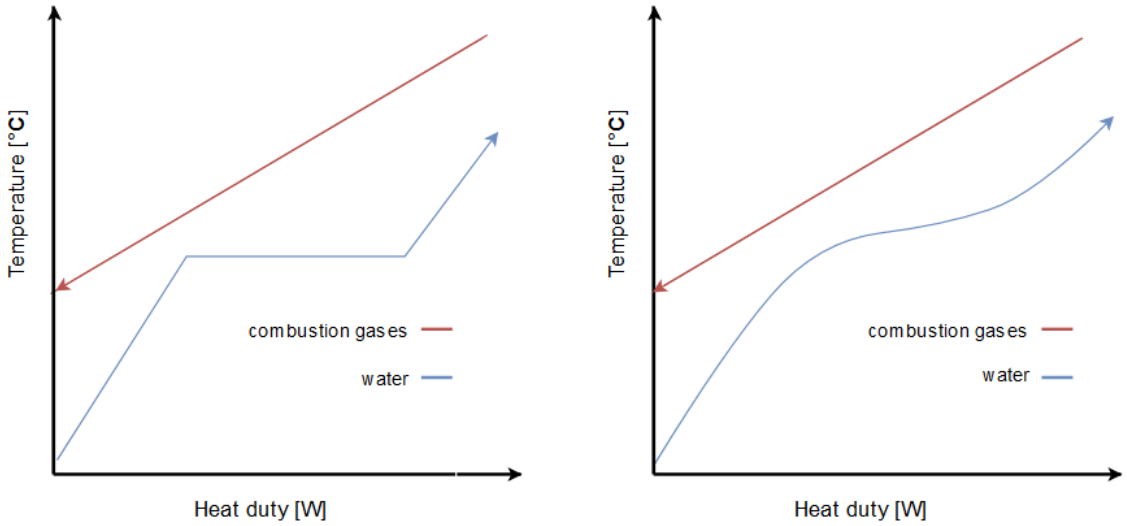

Figure 21. *Simplified situation for the phase change from liquid to steam (left) and the transition to supercritical steam (right) for water. The transition to supercritical steam is drawn according to [16].*

At subcritical conditions the phase change from water to steam occurs at constant temperature leading to a discontinuity in temperature rising as is evident in from Figure 21. The discontinuity in temperature rising leads in noteworthy irreversibility when transferring heat from combustion gases to steam cycle at the HRSG in a combined cycle process. However, if the water in the steam cycle is at supercritical conditions, the addition of heat at the HRSG leads to a continuous temperature rising as is evident in Figure 21. The continuous temperature rising then leads to less irreversibility compared to the phase change of water at subcritical conditions.

In the simulation results it is expected that the recirculation water behaves similarly to the situation illustrated on the right side of Figure 21 at the middle section of the HRSG.

4. CARBON CAPTURE IN POWER GENERATION

The global energy consumption is expected to continue to grow for decades. Fossil fuels are the main source of energy for power generation around the world and there are yet no viable alternatives for such a large scale. As fossil fuel combustion is one of the major mechanisms for CO_2 emissions and hence has a major impact on global warming, it is necessary to find solutions for minimizing the CO_2 emissions caused by fossil fuel combustion in energy generation. Carbon capture and storage (CCS) is a term used to depict a wide range of technologies which are used to prevent or reduce the CO_2 emissions caused by the combustion of fossil fuels, or any other carbon based fuels. The idea with CCS is that the existing infrastructure for fossil fuel combustion could be used for power and electricity generation (albeit with some modifications) by applying the CCS technologies and the CO_2 emissions could be radically diminished. Some of the CCS technologies are already proven to be usable in large scale but mostly they are still economically challenging.

For power generation there are roughly three main methods for carbon capture: post-combustion capture, pre-combustion capture and oxyfuel combustion. These three methods are illustrated in Figure 22. [19]

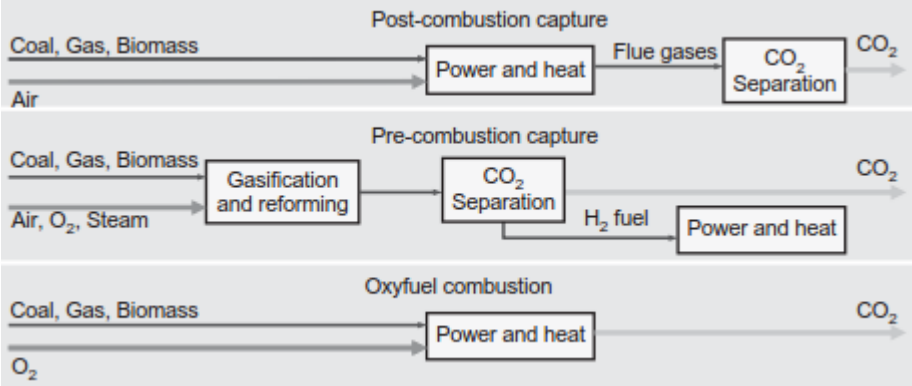

Figure 22. *Methods for CO_2 capture from power generation. [19]*

These three methods illustrated in Figure 22 have their differences but what connects them is that all of them are designed for reducing carbon dioxide emissions involved in energy generation from carbon based fuels. When compared to conventional energy generation without carbon capture, all these methods will lead to diminished carbon dioxide emissions but with the cost of decreased process net efficiency and hence higher costs per unit of energy produced. Each of these carbon capture methods have their

advantages and disadvantages compared to each other and they are briefly summarized in Table 2.

4.1 Pre-combustion capture

Pre-combustion capture is based on producing hydrogen by gasification of fuel (coal, biomass or gas) by means of partial combustion, reforming and water-gas shifting. The achieved product stream is then separated to streams of CO_2 and H_2 from which H_2 is used for power generation and CO_2 can be delivered for further processing or storage. There are several possible ways for CO_2-H_2 separation in use and under development including adsorption based separation as well as membrane and cryogenic separation. Moreover, in the pre-combustion capture method there are still some issues that need further development including optimization of the gasification process and the use of H_2 as the main fuel in a gas turbine system. [19]

4.2 Post-combustion capture

Post-combustion capture is based on separating CO_2 from the combustion gases at the end of the energy generation process before releasing the gases into the atmosphere. For the separation process many technologies are in use or under development. The main advantages of post-combustion capture are that the technologies are proven in large scale applications and the possibility of relatively easily applying them to existing power plants. [19] The disadvantages include the major effect on power plant efficiency (a loss of several %-units) and high costs concerning the operating of the absorption systems in use. [19] CO_2 and H_2 have greater difference in molecular kinetic diameter and molecular weights compared to CO_2 and N_2 (used in post-combustion capture separation process) which make the pre-combustion separation process easier.

4.3 Oxyfuel combustion

Oxyfuel combustion is considered as one of the most promising technologies for CO_2 capture from energy generation in power plants. [3] Oxyfuel combustion is based on the combustion of a carbon based fuel with oxygen as the oxidant instead of air, thus leading to combustion products consisting mainly of CO_2 and H_2O. The high concentrations of CO_2 and H_2O in the combustion products make it possible to separate CO_2 from H_2O by cooling so that most of the water condensates. Then after a relatively simple vapor-liquid separation the vapor component consists of mostly CO_2, which allows further processing of CO_2 for storage conditions or other uses. [3]

The initial requirement for oxyfuel combustion is the separation of oxygen from air. One of the drawbacks of oxyfuel combustion is the energy requirements for the oxygen production processes. Several methods are in use for the separation process and they are

based on adsorption, different kinds of membranes, chemical processes and cryogenic processing. Of these methods, cryogenic processing is the most capable and mature technology for the production of large amounts of high purity oxygen. [20] A recent study examined a novel cryogenic method for air separation, the Nurmia oxygen enrichment method. The study concluded that the Nurmia oxygen enrichment method would be capable of producing 99.6 % pure oxygen at 1 bar while the work needed per mass unit of oxygen product was 350 kJ/kg. [21]

Gas turbine processes with oxyfuel combustion can be operated at near stoichiometric conditions but at least part of the flue gases need to be recycled to the combustion process in order to control the combustion temperature. Without the recycling of the flue gases the combustor outlet temperature would get too high for gas turbines. [3] The basic differences between the introduced carbon capture methods can be seen from Table 2.

Table 2. *Advantages and disadvantages of different combustion methods. Adapted from [19].*

	Advantages	Disadvantages
Pre-combustion capture	Lower energy requirements for CO_2 capture	Temperature and efficiency issues concerning the use of H_2 as the main fuel in a gas turbine system
Post-combustion capture	Fully developed technology and already in use in large scale applications	High parasitic power requirements and efficiency loss
	The possibility to retrofit existing plants	High operational costs for current absorption systems
Oxyfuel combustion	Fully developed air separation technologies in use	Air separation energy requirements for oxygen supply
	Relatively simple CO_2 separation	Impact of oxyfuel combustion on the combustion process

Oxyfuel combustion is the carbon capture method that is used for the process simulation in this thesis. Some of the advantages of oxyfuel combustion are listed in Table 2. One of the main advantages of oxyfuel combustion is the possibility to separate carbon dioxide from the working fluid by relatively simple means. The separation of carbon dioxide from the working fluid will be included in the simulation model studied in this thesis.

The main disadvantages of oxyfuel combustion are also listed in Table 2. The disadvantages of oxyfuel combustion include the energy required for the air separation process for the oxygen supply and the impact of oxyfuel combustion on the combustion process. The air separation process is not simulated in itself but the energy required for oxygen production will be estimated and taken into account in the results section so that the impact of the oxygen supply to the process efficiency is acknowledged. The impact of oxyfuel combustion on the combustion process is taken into account in the simulation model as recycle flows are used to control the temperature in the combustion chamber as the combustion temperature would otherwise get too high due to oxyfuel combustion.

5. INTRODUCTION TO ASPEN PLUS

Aspen Plus is a process optimization software created by Aspen Technology, Inc. It can be used to design, simulate and optimize various industrial processes including gas and steam turbine processes. The large number of unit operations, extensive physical properties database and a capable solver effectively make Aspen Plus a valuable tool for simulating diverse processes. As with many other simulation and modelling software, a sufficient understanding of the relevant physical phenomena is nevertheless required in order to be able to achieve satisfying and reliable results.

When using Aspen Plus the simulation begins in a properties environment. The properties environment is a part of the simulation model where the chemical components as well as the calculation methods for physical properties will be chosen. First the user is required to specify all the chemical components that will appear at any point of the simulation. This means that all the chemical reactions occurring in the simulated process and the reactants of these reactions will need to be determined before running the simulation. Later in the simulation part of the model, all the streams and unit processes will be determined based on the components chosen from the initial component list made in the properties environment. After specifying all the components, the user is required to choose the property methods that will be used to get the thermodynamic properties, such as enthalpies and specific heats, for each of the components.

The simulation environment can be accessed after all the necessary inputs for the properties environment have been specified by the user. The simulation environment is based on the process flowsheet. The process flowsheet will be filled with component blocks which will be connected with material, heat and work streams. The component blocks will be chosen from the Aspen Plus model library, called the Model Palette. Each of the component blocks will be required to be fully specified before running the simulation. Most of the component blocks have multiple ways of specifying the operation conditions but only one of these can be chosen at a time. Also, all the streams that add material to the system need to have their initial conditions fully specified, meaning the chemical composition, temperature, pressure and either mass flow or mole flow of the stream.

The user can finally run the simulation after the process flowsheet is ready and all the necessary details specified. If there are no problems concerning the process and the solution converges, the user can then view the results for any individual component block or stream straight from the flowsheet or optionally view the results section to check all the streams and component blocks in a more compact way. These individual results can be used to check and calculate overall plant performance properties. After a converged solution the user can choose to vary some of the parameters in order to be able to see how

certain changes affect the overall process performance. This could also be achieved by sensitivity analysis or optimization which can be accessed in the simulation environment after a successfully converged solution.

Aspen Plus is a capable software for simulating steady-state combined cycle processes. After getting familiar with the software the user can expect to be able to assemble a combined cycle process in the simulation environment and run the simulation. After a successfully converged simulation the results and the effect of different variables on the overall system can be explored. Nevertheless, it seemed that several problems are likely to arise during simulation, especially for a user not familiar with Aspen Plus beforehand so some patience is required for a complete simulation.

5.1 Initial specifications for simulation

The property method selected for the simulations are the Peng-Robinson equation of state for the gases and IAPWS95 method for steam. The IAPWS95 property method uses the 1995 IAPWS steam table correlations for thermodynamic properties and it is the most accurate property method in the Aspen Physical Property System for thermodynamic properties of water, while the Peng-Robinson equation of state is recommended by Aspen Plus for gas-processing. [22] The Peng-Robinson equation of state was developed by Ding-Yu Peng and Donald Robinson in 1976 and it is defined as [23]

$$p = \frac{R_u T}{V_m - b} = \frac{a\propto}{V_m^2 + 2bV_m - b^2} \tag{5.1}$$

where p is pressure [Pa], R_u [J/(mol K)] is the ideal gas constant, T is temperature [K], V_m is the molar volume. The dimensionless constant α and the coefficients a and b are defined as [23]

$$\propto = (1 + k(1 - T_r^{0.5}))^2 \tag{5.2}$$

$$a = \frac{0.457235 R_u^2 T_c^2}{p_c} \tag{5.3}$$

$$b = \frac{0.077796 R_u T_c}{p_c} \tag{5.4}$$

where T_c and p_c are the temperature and pressure at the critical point, respectively, and T_r is

$$T_r = \frac{T}{T_c} \tag{5.5}$$

and k is [23]

$$k = 0.37464 + 1.54226\omega - 0.26692\omega^2 \tag{5.6}$$

where ω is the acentric factor which is a measure of the non-sphericity of molecules. [24]

The chemical components used in the simulation are presented in Table 3. All the chemical components used in the simulation have to be specified by the user in the property environment in the beginning before any simulation can take place.

Table 3. *The chemical components used in the simulation.*

Component	Chemical formula	Molar mass [g/mol]
methane	CH_4	16.04
ethane	C_2H_6	30.07
propane	C_3H_8	44.10
butane	C_4H_{10}	58.12
carbon dioxide	CO_2	44.01
water	H_2O	18.02
oxygen	O_2	32.00
nitrogen	N_2	28.01
argon	Ar	39.95

Natural gas was chosen as the fuel to be used in the simulations as it is a relatively straightforward but important fuel source for a combined cycle process. The composition of the fuel gas used in the simulations is presented in Table 4.

Table 4. *Chemical composition of the fuel gas. [9]*

Component	Chemical formula	Mole-%
methane	CH_4	98.77
ethane	C_2H_6	0.23
propane	C_3H_8	0.05
butane	C_4H_{10}	0.02
carbon dioxide	CO_2	0.02
oxygen	O_2	0.01
nitrogen	N_2	0.9
Total		100

The heat energy Q_{in} [MW] added into the system by the fuel stream is calculated from

$$Q_{in} = \dot{m}_{fuel} * HHV_{fuel} \tag{5.7}$$

where $\dot{m}_{fuel}$ [kg/s] is the fuel mass flow and HHV_{fuel} [MJ/kg] is the higher heating value of the fuel. The higher heating value for the fuel gas was calculated by the Aspen Plus as HHV_{fuel} = 54.584 MJ/kg.

The amount of oxygen needed for the complete combustion of the fuel gas can be estimated according to the following reactions

$$CH_4 + 2O_2 \rightarrow CO_2 + 2H_2O \tag{5.8}$$

$$C_2H_6 + 3.5O_2 \rightarrow 2CO_2 + 3H_2O \tag{5.9}$$

$$C_3H_8 + 5O_2 \rightarrow 3CO_2 + 4H_2O \tag{5.10}$$

$$C_4H_{10} + 6.5O_2 \rightarrow 4CO_2 + 5H_2O \tag{5.11}$$

and while carbon dioxide and nitrogen components do not react during combustion, the amount of oxygen in the fuel will reduce the overall need of oxygen. According to the Table 4 and the reactions (5.8)-(5.11) for one mole of fuel gas the amount of oxygen needed for stoichiometric combustion is then

$$O_{2\_stoich} = 0.9877 * 2O_2 + 0.0023 * 3.5O_2 + 0.0005 * 5O_2 + 0.0002 * 6.5O_2 - 0.0001O_2 = 1.98715O_2. \tag{5.12}$$

During the simulation a calculator block was used to control the amount of oxygen inserted into the process so that stoichiometric amount of oxygen will be present in the combustion in relation to the amount of fuel. The calculator block will be explained in more detail in Chapter 6.5. The calculator block makes sure that the amount of oxygen inserted into the system would be in agreement with reaction (5.12)

$$n_{O2} = 1.98715 * n_{fuel}. \tag{5.13}$$

6. PROCESS SIMULATION

The main part of this thesis was the simulation of an oxyfuel combined cycle process with the Aspen Plus simulation software. Two scenarios were chosen for the simulation where some of the process parameters were defined beforehand and some were left to be determined during the simulation. First, the process was simulated without the use of argon and the variable parameters were determined through optimization in a way that the process would be as efficient as possible within the chosen boundaries (Case 1). Secondly, the process was simulated again in a similar way with argon introduced to the process (Case 2).

The first case would give an idea of how the process works. The simulation of two similar cases would make it possible to see how certain differences would affect some of the individual aspects of the process as well as the process as a whole. The two cases could be compared with each other as differences were expected in the results. As the process had many things dependent on each other, it was expected that challenges might arise when changing some of the parameters even after a successfully converged initial solution.

6.1 Process description

The process studied in this thesis was an oxyfuel combined cycle from which there are no direct emissions into the atmosphere. The simplified process that was simulated is illustrated in Figure 23. The process has two inlet streams: streams of fuel and oxygen, and two outlet streams: streams of water and carbon dioxide. In Figure 23 the green color represents streams where water is the only component of the stream. Red color represent streams consisting of combustion gases and blue color represents the non-condensable combustion gases. Black color is used to represent various other streams such as the inlet and outlet streams and the cooling flow in the condenser.

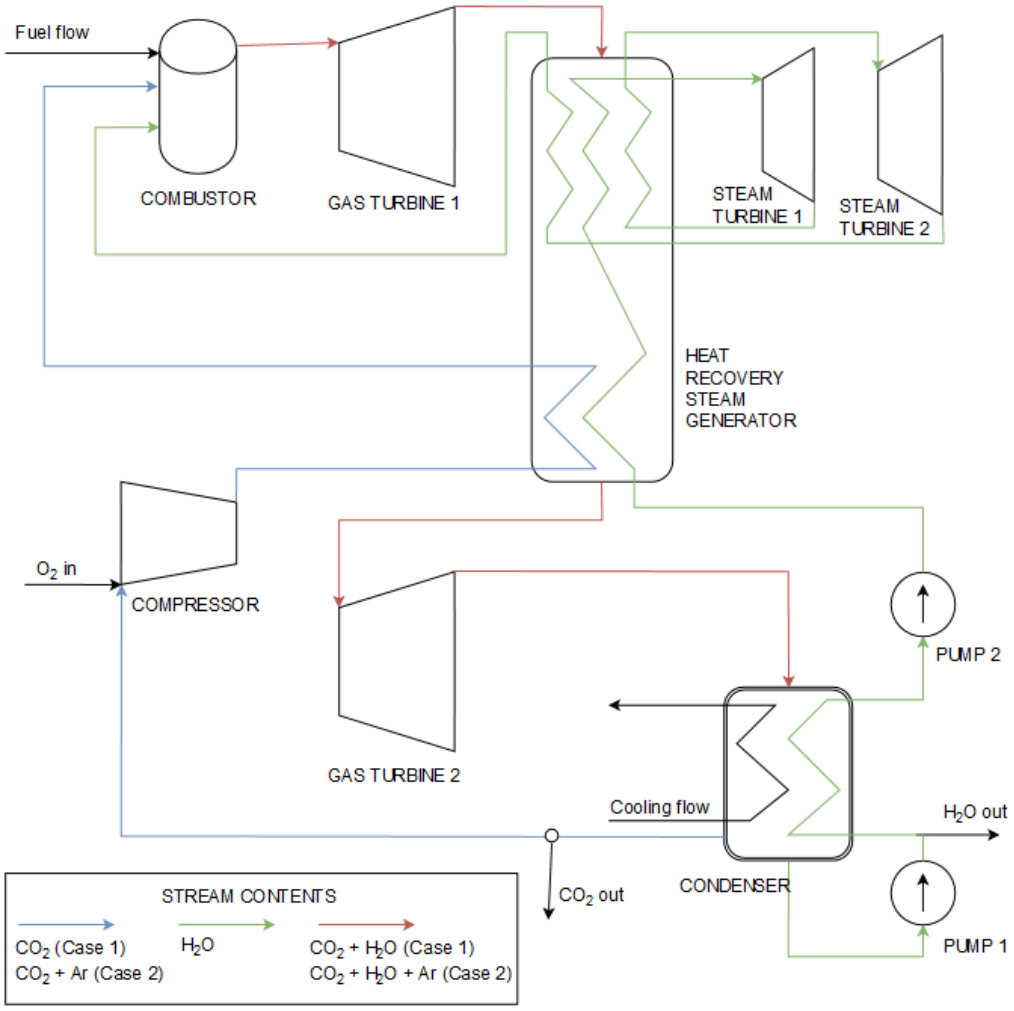

Figure 23. *Simplified process flowsheet for the simulated process.*

The fuel is burned with pure oxygen in the combustor with the presence of steam and the return flow of the non-condensable combustion gases. The presence of these return flows enable maintaining the combustor outlet temperature at a desired level as the oxygen combustion would otherwise lead to temperatures too high for the main gas turbine inlet. After combustion the exhaust gases are expanded in the main gas turbine and led to the heat recovery steam generator (HRSG). In the top section of the HRSG heat is transferred from the combustion gases to the return flow of water (steam) in three separate rounds. At the middle section of the HRSG heat is transferred from the combustion gases to the return flow of water so that the transition from liquid state to gaseous state takes place here in the return flow of water. In the bottom section of the HRSG heat is transferred from combustion gases to both the return flow of water and the return flow of the non-condensable combustion gases. In the bottom section of the HRSG the return flow of water is heated to close to the critical point of water while the return flow of the non-condensable combustion gases is heated before leading it back to the combustor.

After the HRSG, the combustion gases are further expanded to condensation pressure in the second gas turbine after which they are led to the condenser. In the condenser heat is transferred from the combustion gases to both the return flow of water and a stream of cooling flow so that suitable condensation temperature for the combustion gases is reached. At the condenser a major part of the steam component in the combustion gases condensate so that it can easily be separated from the rest of the non-condensable combustion gases in a liquid form. After the condenser the combustion gases have been separated to a stream of liquid water and a stream of non-condensable combustion gases.

After the condenser the water condensate is pressurized and the part of water formed in the combustion is rejected from the process. The rest of the water condensate will make the return flow of water. The return flow of water is then led to reheating in the condenser after which it will be pumped above critical pressure in the second pump. The return flow of water above critical pressure is then heated near the critical temperature in the bottom section of the HRSG and then it goes through the transition from water to supercritical steam in the middle section of the HRSG. At the top section of the HRSG the return flow of water goes through the heat exchanger three times: first it is heated and led to the first steam turbine, then it is reheated again and led to the second steam turbine and finally reheated once more before it is led back to the combustor.

After the condenser the non-condensable combustion gases are led to a separator where the part of carbon dioxide formed in the combustion is removed from the process. The removed carbon dioxide can then be further processed but that is not in the scope of this thesis.

After the part of the carbon dioxide formed in the combustion is rejected, the non-condensable combustion gases are compressed into atmospheric pressure and intercooled after which the oxygen is mixed in. After the addition of oxygen into the non-condensable combustion gases, the mixture is compressed into combustion pressure in three stages with intercooling between the stages. The compressed non-condensable gases are then reheated in the bottom section of the HRSG and led to the combustor. It was chosen that the intercooling between the compressor stages would not be studied in detail in this thesis as it would have made the simulation model even more complicated, but the effect of intercooling on the overall process would still be taken into account.

6.2 Simulated cases

The simulation of the combined cycle process presented in Chapter 6.1 was divided into two separate cases: Case 1 and Case 2. The cases were both based on the same process that was presented in Chapter 6.1 and illustrated in Figure 23. The idea was to maintain minimum differences between the two cases regarding both the process specifications and the process flowsheets so that the results of the simulations would be as comparable as

possible. Case 1 and Case 2 are introduced in more detail in the following Chapters 6.2.1 and 6.2.2.

An inlet temperature of 600 °C for both steam turbines was chosen. One of the main targets for each simulation round was to have the main gas turbine outlet temperature at 605 °C in order to have minimal temperature difference between the hot side gas inlet stream temperature and the cold side steam outlet stream temperature at the top section of the HRSG. According to equation (2.12) for a certain turbine inlet pressure and inlet temperature, the turbine outlet temperature depends on the turbine outlet pressure. For the simulation a design specification block was set to vary the main gas turbine discharge pressure so that the target outlet temperature was reached. The design specification block is explained in more detail in Chapter 6.5.

The mole ratios of the components were left to be decided through the simulations: mainly the mole ratio of carbon dioxide and steam in Case 1 and the mole ratio of argon, carbon dioxide and steam in Case 2. The mole ratios would be determined by varying the amount of return flow of the non-condensable combustion gases for Case 1 and by varying both the return flow of the non-condensable combustion gases and the amount of argon in the process for Case 2.

The condenser pressure and the discharge pressure of the first steam turbine were also left to be decided according to the simulation. The condenser pressure is obviously the same as the discharge pressure of the second gas turbine as can be seen from the simplified process flowsheet in Figure 23. From Figure 23 it can also be seen that the inlet pressure of the second steam turbine is the same as the discharge pressure of the first steam turbine.

6.2.1 Case 1

Case 1 was the simulation scenario with no argon present during simulation. The process flowsheet used for Case 1 is presented in Figure 24. All the component blocks representing different unit operations are named in the process flowsheet with upper case and they are introduced with more detail in Table 8 in Chapter 6.5. Some significant inlet and outlet streams are also named in Figure 24 for demonstrating purposes (with lower case).

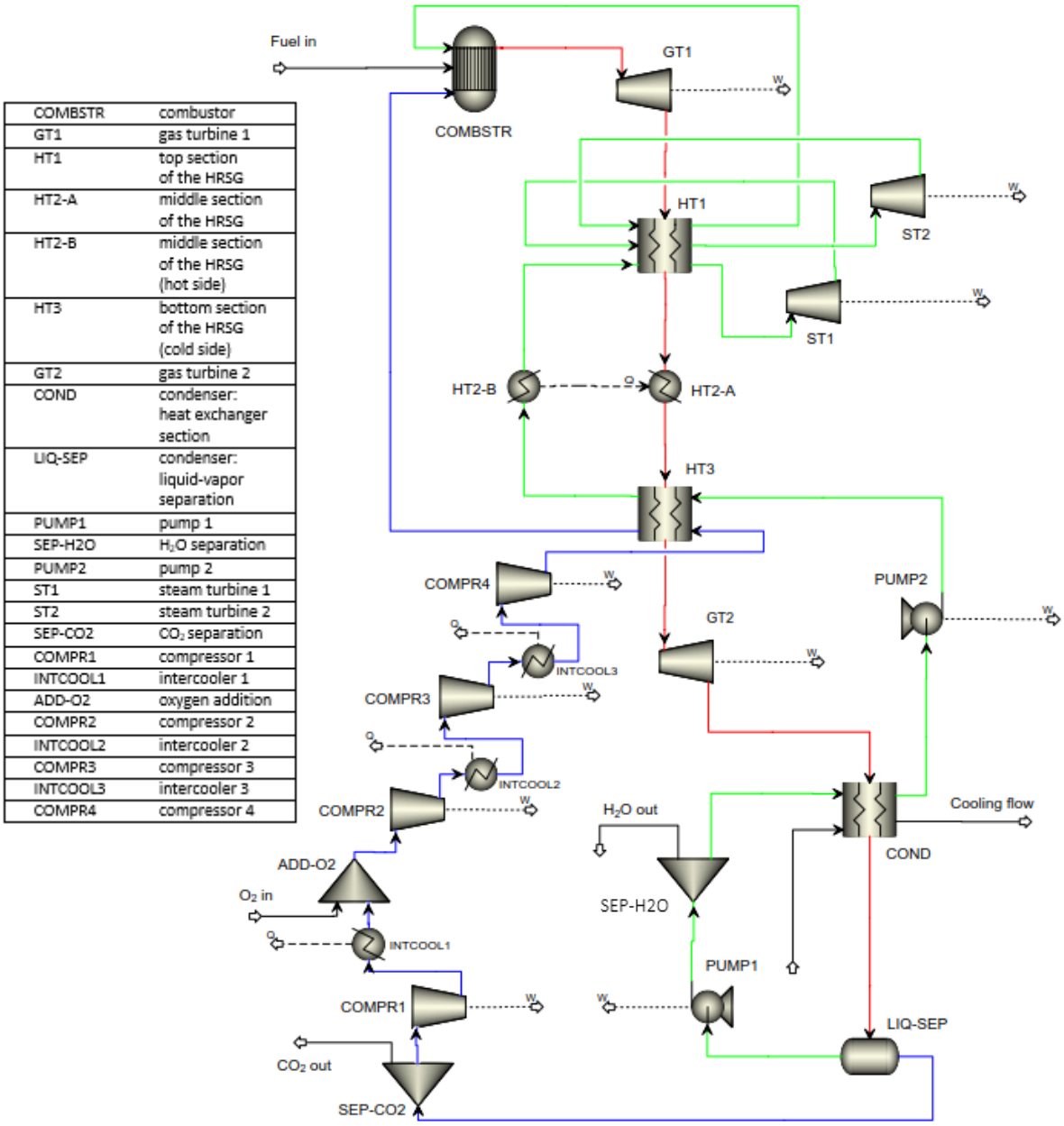

COMBSTR	combustor
GT1	gas turbine 1
HT1	top section of the HRSG
HT2-A	middle section of the HRSG
HT2-B	middle section of the HRSG (hot side)
HT3	bottom section of the HRSG (cold side)
GT2	gas turbine 2
COND	condenser: heat exchanger section
LIQ-SEP	condenser: liquid-vapor separation
PUMP1	pump 1
SEP-H2O	H_2O separation
PUMP2	pump 2
ST1	steam turbine 1
ST2	steam turbine 2
SEP-CO2	CO_2 separation
COMPR1	compressor 1
INTCOOL1	intercooler 1
ADD-O2	oxygen addition
COMPR2	compressor 2
INTCOOL2	intercooler 2
COMPR3	compressor 3
INTCOOL3	intercooler 3
COMPR4	compressor 4

Figure 24. *The process flowsheet for Case 1.*

The coloring of the streams in Figure 24 is the same as with the simplified process in Figure 23. The dashed lines in the process flowsheet in Figure 24 represent heat and work streams with the more coarsely dashed line representing heat streams and the more densely dashed line representing work streams, respectively. In Figure 24 all the heat and work streams are aimed outwards but Aspen Plus takes the direction of the streams into account by setting a negative sign for work produced in a component block and a positive sign for work required. A similar principle is used with the heat streams as for heat produced in a component block will be positive and heat removed will be negative.

In the process flowsheet the condenser is divided into two sections for practical simulation reasons where the first part of the condenser is a heat exchanger in which the combustion gases reject heat in order to reach the desired condensation temperature and the second part of the condenser separates the liquid and gaseous components of the combustion gases. After the condensed water has been separated from the non-condensable combustion gases, the non-condensable combustion gases are led to a separator where a fraction of the stream is rejected out of the system. This rejected stream has the same composition as the original flow of the non-condensable combustion gases before the separation.

In order for the combustion gases to reach the desired outlet temperature of 605 ºC after the expansion in the main gas turbine, a lower discharge pressure was expected in Case 1 when compared to Case 2 with argon. The necessary discharge pressure for the main gas turbine would be solved through simulations. Also, the mole ratio of carbon dioxide and steam in the combustion gases would be found out so that all the requirements for the process would be fulfilled while trying to maximize the thermal efficiency of the process at the same time. The results of the Case 1 simulation will be presented in the Chapter 7.

6.2.2 Case 2: with argon

Case 2 was a simulation scenario where argon was introduced to the process. The process flowsheet used for Case 2 is presented in Figure 25 and it is exactly the same as the one used for Case 1 with minor exceptions. The separation of carbon dioxide from the process in Case 2 requires an additional mixer to be used in the process flowsheet. The process specifications were the same as with Case 1 with some small exceptions. The argon component in the return flow of the non-condensable combustion gases would lead to higher temperatures after the last compression stage so the combustor inlet temperature for the return flow of the non-condensable combustion gases was set to 320 ºC instead of 300 ºC used in Case 1.

Due to the presence of argon in the combustion gases, it was expected that higher discharge pressure for the main gas turbine would be sufficient to reach the desired outlet temperature of 605 ºC after the expansion in the main gas turbine. A higher pressure would lead to lower capital costs concerning both the HRSG and the gas turbine as higher discharge pressure for gas the first gas turbine would mean smaller pressure difference between the exhaust gases and the environment and thus lower costs concerning the piping for the HRSG. Higher discharge pressure would also mean smaller gas turbine and lower capital costs because of that too. A discharge pressure close to the atmospheric pressure was the target for Case 2. Similarly to Case 1, the mole ratio of argon, carbon dioxide and steam in the combustion gases would be found out through simulation while fulfilling all the requirements and trying to maximize the thermal efficiency of the system at the same time.

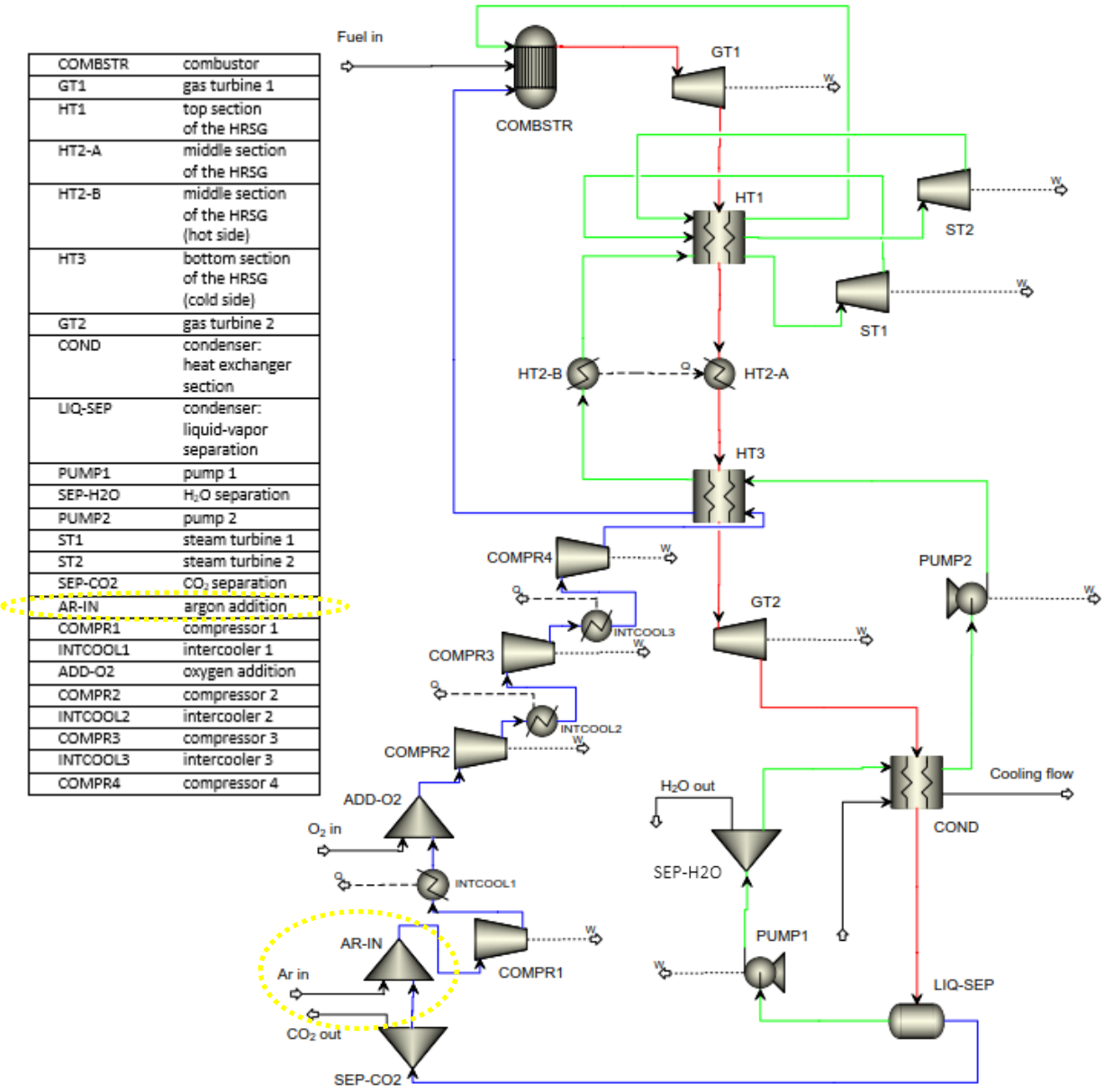

Figure 25. *The process flowsheet for Case 2. The difference between Case 1 and Case 2 process flowsheets is highlighted in yellow.*

The coloring of the streams in Figure 25 is the same as it is in Figure 24 and Figure 23. The difference in the process flowsheets for Case 1 and Case 2 is highlighted in yellow in Figure 25. The additional inlet stream is an inlet stream of argon. In practice the argon would be added into the system as a minor part of the oxygen inlet stream. The added argon would then accumulate into the process and the part of carbon dioxide to be rejected would be separated from the non-condensable combustion gases. However, during simulation the rejection of carbon dioxide is performed by a simple separator so the rejected stream of carbon dioxide is a mixture of carbon dioxide and argon. The additional inlet stream of argon in the process flowsheet adds back into the process the amount of

argon rejected with the carbon dioxide, hence maintaining the mass balance. The estimated separation work needed for the separation of carbon dioxide from the mixture of the non-condensable combustion gases will be taken into account in the results section in Chapter 7.

6.3 Process specifications for the simulation

For the simulation some parameters were fixed while some were left to be defined through optimization. The chosen fixed parameters are presented in Table 5.

Table 5. *Process specifications for the simulation.*

Parameter	Value	Unit
Fuel inlet temperature (natural gas)	20	ºC
Combustion pressure	20	bar
Turbine inlet temperature	1400	ºC
Steam temperature (the top section of the HRSG)	600	ºC
Supercritical steam temperature (the middle section of the HRSG)	450	ºC
Steam temperature (the bottom section of the HRSG)	350	ºC
Non-condensable combustion gases combustor inlet temperature (Case 1)	300	ºC
Non-condensable combustion gases combustor inlet temperature (Case 2)	320	ºC
Recirculation water pressure after the first pump	1	bar
Recirculation water pressure after the second pump	300	bar
Water temperature after the condenser	80	ºC
Condensation temperature	18	ºC
Condenser cooling flow pressure	1	bar
Condenser cooling flow inlet temperature	10	ºC
Condenser cooling flow outlet temperature	80	ºC
Compression pressure: compressor 1	1	bar
Compression pressure: compressor 2	2	bar
Compression pressure: compressor 3	4	bar
Compression pressure: compressor 4	20	bar
Intercooling: degrees of superheating for compressed gas	10	ºC
Inlet pressure for oxygen	1	bar
Inlet temperature for oxygen	20	ºC

For the simulation it was assumed that natural gas would be available at 20 ºC and at the combustion pressure of 20 bar. The quantity of the fuel inlet stream would be varied so that the turbine inlet temperature would remain at 1400 ºC.

A turbine inlet temperature of 1400 ºC was chosen as it has been used in previous research [25, 26] and is at the upper scale of turbine inlet temperatures currently in use [8]. The main barrier for high turbine inlet temperatures are turbine blade material limitations. Thermal barrier coatings and turbine blade cooling are used to make it possible to use turbine inlet temperatures around 1400 ºC and higher. The effect of cooling was not taken into account during this study as it would have been difficult to estimate it for the set of conditions used in the simulation.

Turbine inlet temperature (which is the same as the combustor outlet temperature) was an important parameter chosen for the process. As there were return flows of steam and the non-condensable combustion gases injected into the combustor it was clear that any change in the conditions of these flows (mainly the stream mole flows or the stream temperatures) would affect the combustor outlet temperature. Thus a design specification block was applied to maintain the chosen turbine inlet temperature regardless of the changes of the two extra streams into the combustor. The design specification block will be explained in more detail in Chapter 6.5. The design specification block was programmed to vary the fuel flow so that the turbine inlet temperature would remain as planned. The calculator block mentioned earlier would then make sure that the amount of oxygen inserted into the system would match the varied fuel flow in all situations.

Steam temperature at the top section of the HRSG was specified at 600 ºC as it is a turbine inlet temperature that current supercritical steam turbines can work with [13, 14].

The recirculation water is at supercritical pressure when it enters the bottom section of the HRSG. In the bottom section of the HRSG the recirculation water will be heated to near the critical point and then when it absorbs enough heat from the combustion gases at the middle section of the HRSG it will transition into supercritical steam. The bottom section of the HRSG was specified in a way that the recirculation water outlet temperature would be 350 ºC which is close to the critical temperature. The middle section of the HRSG was where the recirculation water would then go through the transition to supercritical steam. In order to let the recirculation to fully go through the transition into supercritical steam in the middle section of the HRSG, an outlet temperature of 450 ºC was specified.

Reheating of the recirculation flows before returning them to the combustor reduces the amount of fuel required. At the bottom section of the HRSG the temperature of the hot gases limits the available reheat temperature for return flow of the non-condensable gases. A reheat temperature of 300 ºC was defined for Case 1 and 320 ºC for Case 2. The difference in the composition of the non-condensable gases leads to higher temperatures after the compression for Case 2. Thus the reheat temperature was set slightly higher for Case 2.

The first pump was specified so that it would pressurize the condensed water to 1 bar after which the amount of water produced in the combustion process would be rejected. The second pump would then pressurize the recirculation water to supercritical pressure of 300 bar which is a pressure level that current supercritical steam turbines can work with [13, 14].

A reheat temperature of 80 ºC at the condenser was defined for the return flow of the recirculation water, and the same temperature was chosen for the cooling flow condenser outlet temperature.

The compression of the return flow of the non-condensable gases was simulated in four stages. The first compressor would compress the gases to a pressure of 1 bar, the second one to 2 bar, the third one to 4 bar and the fourth one to the combustion pressure of 20 bar. Intercooling was used in the simulation to reduce the compression work required with heat rejection between the compression stages. A total of three intercooling stages where then used for the four compression stages. The amount of heat that could be rejected between the compression stages depends on the gas composition, temperature and quantity. In order to reject a considerable amount of heat between the compression stages while also making sure that no problems would arise when the gas composition, temperature and quantity would change during different simulation rounds, a method of specifying a degree of superheating after each intercooling stage was chosen. If too much heat would be rejected from the non-condensable gases during simulation, the vapor fraction of the non-condensable gases could slip below 1. By specifying 10 degrees of superheating for the non-condensable gases after each intercooling stage would make sure that the non-condensable gases would remain gaseous at all situations during simulation.

The air separation process needed to produce the required oxygen flow was not included in the simulation used for Case 1 and Case 2 but the energy required for the oxygen produced would be taken into account in the results in Chapter 7. The oxygen inlet stream was specified according to [21] at 1 bar with a composition of 100 molar-% oxygen, at the temperature of 20 ºC. The combustion was simulated in stoichiometric conditions so the quantity of the oxygen inlet stream was varied in order to ensure stoichiometric conditions during the different simulation rounds.

The amount of water produced in the combustion process was rejected from the process but the amount of water returned to the process was not defined beforehand. The HRSG would set limits to the ratio of the amount of the recirculation water to the amount of combustion gases. There would be problems in the HRSG if the ratio of recirculation water to combustion gases would not be balanced. If too much combustion gases in relation to recirculation water, the combustion gas HRSG outlet temperature would be unnecessary high. Then again if too much recirculation water in relation to combustion gases, there would be not enough heat available in the combustion gases in the HRSG. In order to control this, it was defined that the combustion gas temperature at the outlet of

the middle section of the HRSG would be 5 degrees higher than the recirculation water temperature at the inlet of the middle section of the HRSG.

Condenser cooling flow was set to a pressure of 1 bar with an inlet temperature of 10 ºC. A condensation temperature of 18 ºC was chosen for the gases [26], thus a temperature difference of 8 ºC between the cooling flow inlet stream and the combustion gases outlet stream was defined. The cooling flow stream was defined as water with a condenser outlet temperature of 80 ºC and the mass flow of the cooling flow stream was varied in order to reach these specifications.

For the simulation of turbines, compressors and pumps the following isentropic efficiencies were chosen and are presented in Table 6.

Table 6. *Turbine, compressor and pump isentropic efficiencies.*

Component	η_s
Gas turbine 1	0.92
Gas turbine 2	0.90
Steam turbine 1	0.92
Steam turbine 2	0.92
Compressors 1-4	0.89
Pumps	0.80

For turbines and compressors a mechanical efficiency of 0.99 was chosen while an electrical efficiency of 0.99 was chosen for the pumps.

6.4 Optimization

Aspen Plus Optimization was used to find out the optimum set of parameters with which the highest thermal efficiency for each of the cases would be reached. The Optimization tool would make use of a fully defined and complete process to allow the user to try to optimize the process in a desired way. The Optimization tool requires one main parameter to be either maximized or minimized and then a set of other parameters are required to be chosen by the user. The Optimization tool then uses this set of parameters and varies them in order to find the best combination of values for the set of parameters with which the optimum maximum or minimum value for the main parameter would be possible.

For both cases the maximization of the thermal efficiency of the process was chosen as the main parameter for the Optimization tool. A set of three variable parameters was chosen for the optimization in Case 1 and a set of four parameters was chosen for the optimization in Case 2. In Case 1 the set of parameters chosen included the discharge

pressure of the second gas turbine, the discharge pressure of the first steam turbine and the amount of the non-condensable combustion gases recirculating in the process after the rejection of carbon dioxide from the process. For the optimization of the process in Case 2 the set of parameters to be varied was the same as in Case 1 with one additional parameter that was the amount of argon in the process.

The Optimization tool also allows the user to set constraints for the optimization process so that poor, unwanted or impractical optimization results could be avoided. The constraints can be minimum or maximum value restrictions for streams or component blocks all around the process flowsheet, for example. The Optimization tool will then respect the constraints when varying the set of parameters that were defined by the user.

Three constraints were used for the optimization of Case 1 and four constraints were used for the optimization of Case 2. The optimization constraints used in the simulation are summarized in Table 7.

Table 7. *The optimization constraints used in the simulation for Case 1 and Case 2. The 'x' marks the constraints used in each case.*

Constrained parameter	Limit value	Unit	Case 1	Case 2
Gas turbine 1 power	$P \geq 300$	MW	x	x
Gas turbine 1 discharge pressure	$p \geq 0.9$	bar	-	x
Gas turbine 2 outlet temperature	$T \geq 90$	ºC	x	x
Gas turbine 2 discharge pressure	$p \geq 0.1$	bar	x	x

One of the constraints was to set the main gas turbine power to 300 MW, with a tolerance, so that the two cases could be more comparable with each other. Another constrain was to set a minimum value for the second gas turbine outlet temperature in order to make sure that there would be no temperature crossovers in the condenser at low condensation pressures. A minimum condensation pressure of 0.1 bar was chosen for the both cases as the third common constraint.

For Case 2 the idea was that the presence of argon in the working fluid would make it possible that a discharge pressure close to the atmospheric pressure would be sufficient. Thus a fourth constraint was set for the optimization of Case 2 in which a minimum discharge pressure of 0.9 bar was defined for the gas turbine 1.

6.5 Component modelling in Aspen Plus

Each of the component blocks used in the simulation will use user-defined operation specifications and material, heat and work stream inputs in order to calculate relevant

material, heat and work stream outputs. As each of the component blocks are connected with each other through the streams, an overall solution will be obtained. The component blocks used in the simulation are presented in Table 8, where the component blocks are listed with short explanations of their respective functions on the process.

Table 8. *The component blocks used in the simulation.*

Component	Function	Other notes	Block names
Compr	Pressure changer	Used for turbines and compressors	Turbines: GT1, GT2, ST1, ST2 Compressors: COMPR1, COMPR2, COMPR3, COMPR4
Flash2	Two-phase separator	Separation of liquid phase and gas phase	LIQ-SEP
Heater	Heater	Single stream heat exchanger	HT2-A, HT2-B, INTCOOL1, INTCOOL2, INTCOOL3
MHeatX	Heat exchanger	Multistream heat exchanger	HT1, HT3, COND
Mixer	Mixer		ADD-O2, AR-IN
Pump	Pump		PUMP1, PUMP2
RGibbs	Combustor		COMBSTR
FSplit	Separator		SEP-H2O, SEP-CO2

The component blocks representing the unit operations used in the simulation will be introduced briefly next.

Compressors

The compressor in the process flowsheet was simulated in four compression stages with intercooling between the stages by using the block Compr for compression and the block Heater for intercooling. A Heater block represents a single stream heat exchanger. A fully defined Heater block needs a material inlet and outlet stream and user-defined operating conditions. The Heater block uses these user-defined operating conditions and the inlet stream conditions to calculate the outlet stream conditions as well as the required (or produced) heat stream out of the Heater block. There are different sets of two operating conditions to be chosen from. Pressure and degrees of superheating were chosen in this simulation as the specified operating conditions. All the Heater blocks were chosen to have the same defined operating conditions: 0 bar for pressure indicating zero pressure drop during intercooling and a degree of superheating of 10 degrees. Degrees of superheating was chosen as one of the defined operating conditions to maintain high

levels of cooling and to maintain fully gaseous stream at all times even with changing stream conditions during simulations.

The Compr block can be used to model either a compressor or a turbine. To model a compressor, it was necessary to choose “compressor” as the type in the setup of Compr block. A discharge pressure was defined for all the compressors as the outlet specification as well as isentropic and mechanical efficiencies. The Compr block setup window can be seen in Figure 26.

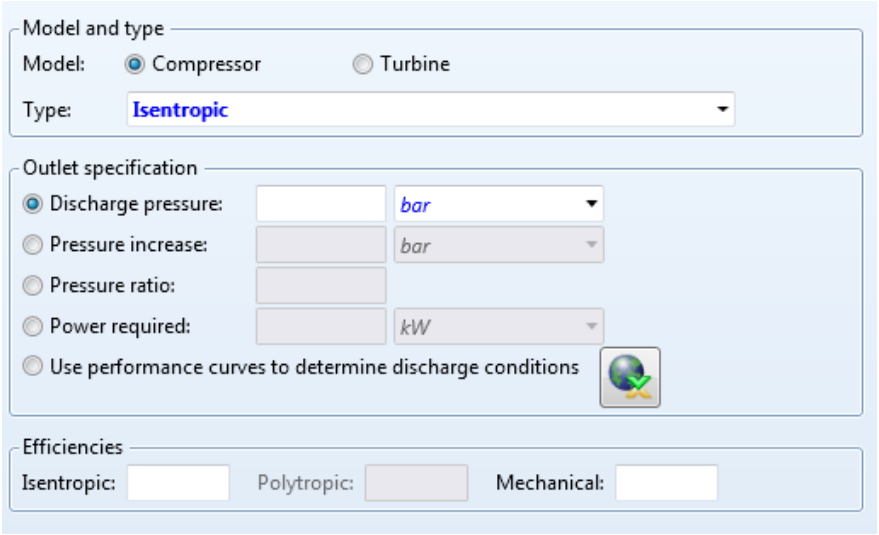

Figure 26. *The Compr block setup window.*

Four Compr component blocks were used in the process simulation: COMPR1, COMPR2, COMPR3 and COMPR4 and three Heater blocks were used for the intercooling: INTCOOL1, INTCOOL2 and INTCOOL3. These component blocks can be found in the process flowsheets in Figure 24 and Figure 25.

Combustor

The combustor was simulated by using a component block RGibbs. The RGibbs block is an ideal reactor that can be used without the need for detailed stoichiometry or yield. [22] RGibbs minimizes the Gibb’s free energy to calculate the equilibrium composition of the mixture at the combustor outlet as well as the heat released to the fluid, hence the outlet temperature of the mixture will be solved. The RGibbs block can take one or more input material streams and one or more output material streams and an optional input or output heat stream. The RGibbs block is fully specified when two out the three of the following operating conditions are set: pressure, temperature and heat duty. For this simulation heat duty and pressure were chosen as the defined operating conditions and both were set to zero to indicate zero pressure drop during the combustion and zero heat duty to indicate

no heat loss from the combustion, in other words adiabatic combustion. An RGibbs block COMBSTR was used in the simulation and it can be found in the process flowsheets in Figure 24 and Figure 25.

Gas turbines

In the simulation the gas turbines were also modelled with the Compr blocks. The setup was identical to that of compressors as seen in Figure 26 with the exception that "turbine" was chosen as the type in the setup. Isentropic and mechanical efficiencies were defined to account for non-ideal expansion. Two Compr blocks were used in the simulation for the modelling of gas turbines: GT1 and GT2, and they can be found in the process flowsheets in Figure 24 and Figure 25.

Steam turbines

The steam turbines were modeled the same way as the gas turbines. Two Compr blocks were used in the simulation for the modelling of steam turbines: ST1 and ST2, and they can be found in the process flowsheets in Figure 24 and Figure 25.

Heat recovery steam generator

The recovery heat steam generator (HRSG) was divided in the process flowsheet into three sections. In the first section of the HRSG heat was transferred from the gas turbine exhaust gas into three streams of steam. In the middle section heat was transferred from the gas turbine exhaust gas into one stream of steam only and in the third section heat was transferred from the gas turbine exhaust gas into one stream of steam and one stream of the returning flow of the non-condensable combustion gases. The first and third section of the HRSG were modeled as multistream heat exchangers (an MHeatX block in Aspen Plus): HT1 and HT3, and the middle section as a single stream heat exchanger (a Heater block) with two separate Heater component blocks: HT2-A and HT2-B. These component blocks can be found in the process flowsheets in Figure 24 and Figure 25.

A MHeatX component block can be used to model the rejection of heat from one hot stream to multiple cold streams. The MHeatX blocks are fully defined when all but one of the streams are specified in one of the available methods. In this simulation the MHeatX blocks at the first and third section of the HRSG were specified so that the outlet temperatures for the cold streams were defined. With the cold streams defined, the MHeatX block will calculate the required heat flow from the hot stream to the cold streams and thus solving the outlet temperature of the hot stream after the heat rejection.

The Heater blocks used in the middle section of the HRSG were similar to the ones used for intercooling in the compression. Two Heater blocks were used in the middle section of the HRSG. One of them (HT2-B) would solve the amount of heat needed to achieve the desired steam conditions at the outlet of the middle section of the HRSG. The two Heater blocks were connected so that the hot gas turbine exhaust gases would then reject

the same amount of heat in the gas side Heater block (HT2-A). The steam side Heater block (HT2-B) was defined be specifying zero pressure drop and by specifying the steam outlet to a point where the steam would be supercritical. With these operating conditions the Heater block HT2-B would calculate the necessary heat input to the steam side. As the two Heater blocks were connected with a heat stream between them, this heat input required would automatically serve as one of the two operating conditions to the gas side Heater block (HT2-A), the other one being zero pressure drop also. This connection of the two Heater blocks would enable solving the outlet conditions for the gas side of the middle section of the HRSG after rejecting the necessary amount of heat to the steam side.

Condenser

The condenser was modelled in two sections for more practical simulation. The first section of the condenser was a heat exchanger where the hot combustion gases would reject enough heat to reach the desired condensation temperature. The second section of the condenser was a flash separator where the liquid and gaseous components of the combustion gases would be separated. The first section of the condenser was modelled as a multistream heat exchanger by component block MHeatX and the liquid-vapor separation in the second section was modelled by a Flash2 component block.

The MHeatX block was specified in a way that the combustion gases would reject heat to two cold streams (a stream of recirculation water and a stream of cooling flow) so that the multistream heat exchanger outlet temperatures were set for the combustion gases and the recirculation water while the cooling flow outlet temperature would be solved. During simulations the cooling flow mass flow was varied so that the desired cooling flow outlet temperature would be reached. The first section was modelled in the process flowsheet by the MHeatX component block named COND and it can be found in the process flowsheets in Figure 24 and Figure 25.

After the first section of the condenser the combustion gases would then be in a state where part of the steam component had been condensed so the combustion gases would consist of two phases: gas and liquid. After the first section, the combustion gases would enter a separator component block. The separator has one inlet stream and two outlet streams. The separator would separate the two-phase inlet stream into two outlet streams: one gaseous stream and one liquid stream. The Flash2 separator was named in the process flowsheet as the LIQ-SEP and it can be found in the process flowsheets in Figure 24 and Figure 25.

Pumps

A component block for pumps was available for simulating the pumps in the process flowsheet. The pump component block is designed to handle a single liquid phase. The pump block requires the user to specify the discharge pressure and isentropic and

electrical efficiencies with which the pump block calculates the power required. The pump block inlet stream conditions (temperature, pressure) affect the pump block outlet conditions and the power required for pumping. The pump inlet conditions were not defined by the user but they would be determined by the previous component or operation on the process flowsheet. Two pump blocks, PUMP1 and PUMP2 were used in the simulation and they can be found in the process flowsheets in Figure 24 and Figure 25.

Mixers and separators

FSplit and Mixer blocks were used to separate and mix streams during the simulation. The component block used for simple separation, FSplit, has a simple unit operation where one inlet stream can be divided into two outlet streams. These outlet streams will have identical state (chemical composition, temperature, pressure) with the inlet stream. For an FSplit block at least one of the outlet streams need to be specified by the user and there are several ways to do that. In this simulation the FSplit blocks were defined by specifying the flow rate of one of the outlet streams. The FSplit block would then simply subtract this specified outlet stream from the inlet stream and the rest would make up the other outlet stream. Two FSplit blocks were used in the simulation, SEP-H2O block for separating a stream of water into two streams and SEP-CO2 block separating a stream of the non-condensable combustion gases into two streams. For both of these FSplit blocks the flow rate of the stream that would be returned to the process was specified while the leftover stream would be taken out of the process.

A Mixer block can have multiple inlet streams and it combines them to produce a single outlet stream by simply completing material balance. A Mixer block, ADD-O2, was used to mix an oxygen stream with the non-condensable combustion gases. In Case 2 another Mixer block, AR-IN, was also used to add back the part of argon removed from the system with the rejected stream of carbon dioxide. The Mixer and FSplit component blocks can be found in the process flowsheets in Figure 24 and Figure 25.

Design specification blocks and calculator blocks

A design specification block is a component that can be used in the flowsheet to help constrain some of the process parameters. The design specification block monitors a chosen variable on the process flowsheet and can then manipulate another variable on the process flowsheet according to user-defined specifications. The user defines a target value for the variable under monitoring and the design specification block then varies the manipulated variable iteratively until the variable under monitoring achieves the desired target value. A few design specification components were used in the simulation. One design specification block was used to control the combustor outlet temperature which is the same as the turbine inlet temperature for gas turbine 1 by varying fuel flow. Another design specification block was used to control the exhaust temperature for gas turbine 1 by varying the gas turbine 1 discharge pressure. One design specification block was also

used to make sure that there were no issues with the heat recovery steam generator so that there would be no temperature crossovers between the hot and cold flows, for example.

The design specification block operates in a feed-back fashion, but a calculator block on the other hand is a similar component that operates in a feed-forward fashion. The calculator component uses user-defined calculations that can use values from any part of the process flowsheet to control certain chosen variables. One calculator component block was used in the simulation to control the oxygen flow into the process in relation to the fuel flow. The calculator block used was configured in a way that it made sure that the oxygen flow would match the fuel flow according to equation (5.13).

6.6 Problems

Several challenges occurred during simulation. As the process flowsheet is somewhat complex with many of its sections and unit operations dependent on each other, problems occurred in different parts of the process flowsheet when varying some parameters, especially in the beginning of the simulations. The problems varied from temperature crossovers in heat exchangers to unsuitable two-phase flows in compressors, pumps or turbines and from solution convergence problems to incorrect component block specifications by the user. Some of the problems were overcome by trial and error while some could be resolved by putting design specification blocks or calculators into operation.

7. RESULTS AND DISCUSSION

The results of the simulations will be presented in this chapter. The main performance characteristics of the process are presented for Case 1 and Case 2 with essential tables and figures. The gas turbine discharge pressures and pressure ratios are presented in Table 9. The discharge pressure for the gas turbine 1 was calculated during the simulations so that all the process specifications and criteria was fulfilled. The gas turbine 2 discharge pressure was optimized for both cases. The inlet pressure for the first steam turbine was set to 300 bar according to the process specifications in Table 5. The discharge pressure for the second steam turbine was set to 20 bar as the combustion pressure. The pressure ratios for the turbines are calculated according to equation (2.13).

Table 9. *The optimal discharge pressure for the turbines.*

Parameter	Case 1	Case 2	Unit
Gas turbine 1 discharge pressure	0.230	0.963	bar
Gas turbine 1 pressure ratio	87.0	20.8	-
Gas turbine 2 discharge pressure	0.162	0.341	bar
Gas turbine 2 pressure ratio	1.42	2.82	-
Steam turbine 1 discharge pressure	89.62	87.98	bar
Steam turbine 1 pressure ratio	3.3	3.4	-
Steam turbine 2 pressure ratio	4.5	4.4	-

In Table 9 the main difference between Case 1 and Case 2 is the pressure ratio for the gas turbine 1. Here it is important to remember that the inlet pressure was 20 bar in both cases so the difference in the pressure ratios is due to the difference in the discharge pressures which can also be seen in Table 9. Then again, in order to achieve the desired gas turbine 1 outlet temperature of 605 ºC, a higher pressure ratio was expected in Case 1 because of the lower ratio of specific heats of the working fluid.

Some of the streams at the key points of the process are presented in the following tables. The state and composition of the combustion gas after combustion is presented in Table 10.

Table 10. *The state and composition of the combustion gas after combustion.*

	Case 1	Case 2	Unit
Temperature	1400	1400	ºC
Pressure	20	20	bar
Vapor fraction	1	1	-
Molar flow	7.3	10.9	kmol/s
Mass flow	242.3	377.3	kg/s
Mole fraction CO_2	57.6	20.8	%
Mole fraction H_2O	41.9	27.9	%
Mole fraction Ar	0.0	51.1	%
Mole fraction N_2	0.5	0.2	%

In Case 2 argon was a major component in the process working fluid. Table 10 shows that the combustion gases include a molar fraction of 51.1 % of argon. The argon component allows the use of significantly lower pressure ratio for the first gas turbine as was seen in Table 9: the pressure ratio is 20.8 for the first gas turbine in Case 1 compared to a pressure ratio of 87.0 in Case 2. Such a large difference between the pressure ratios indicate that a smaller gas turbine is sufficient when argon is part of the working fluid. Lower capital costs can be expected with a smaller gas turbine. Lower discharge pressure leads to higher specific volume for the exhaust gases which is why the lower the discharge pressure, the bigger the low-pressure part of the gas turbine has to be.

Most of the water in the combustion gases is liquefied in the condenser and separated from the non-condensable gases. Table 11 shows the state and composition of the non-condensable combustion gases after the separation of liquid water at the condenser.

Table 11. *The state and composition of the non-condensable combustion gases after the condenser.*

	Case 1	Case 2	Unit
Temperature	18	18	ºC
Pressure	0.162	0.341	bar
Vapor fraction	1	1	-
Molar flow	4.7	8.3	kmol/s
Mass flow	195.6	329.8	kg/s
Mole fraction CO_2	89.0	27.4	%
Mole fraction H_2O	10.2	4.9	%
Mole fraction Ar	0.0	67.5	%
Mole fraction N_2	0.8	0.2	%

From Table 11 it can be seen that in Case 1 the working fluid contains 89.0 molar-% of carbon dioxide and 10.2 molar-% of steam after the separation of liquid water in the condenser. Table 11 shows that at the same point of the process in Case 2 the working fluid contains 67.5 molar-% of argon and 4.9 molar-% of steam. The amount of carbon dioxide formed in the combustion needs to be rejected from the process for a complete mass balance in the system. Table 12 shows the state and composition of the non-condensable combustion gases after the rejection of part of the carbon dioxide from the process.

Table 12. *The state and composition of the non-condensable combustion gases after the carbon dioxide rejection*

	Case 1	Case 2	Unit
Temperature	18	18	ºC
Pressure	0.162	0.341	bar
Vapor fraction	1	1	-
Molar flow	4.2	7.7	kmol/s
Mass flow	173.1	306.6	kg/s
Mole fraction CO_2	89.0	23.2	%
Mole fraction H_2O	10.2	4.1	%
Mole fraction Ar	0.0	72.7	%
Mole fraction N_2	0.8	0.2	%

From Table 12 it can be seen that in Case 1 the composition of the non-condensable gases is the same before and after the rejection of carbon dioxide, which is due to the fact that in Case 1 the rejection of carbon dioxide was modelled simply by subtracting a fraction of the stream and rejected from the process. On the other hand, in Case 2 the composition changes as the part of carbon dioxide formed in combustion is separated from the mixture of non-condensable gases and the rest of the non-condensable gases are then returned into the process. The composition of the rejected stream of carbon dioxide is presented in Table 13.

Table 13. *The composition and state of rejected stream of carbon dioxide.*

	Case 1	Case 2	Unit
Temperature	18	18	ºC
Pressure	0.162	0.341	bar
Vapor fraction	1	1	-
Molar flow	0.547	0.579	kmol/s
Mass flow	22.5	23.1	kg/s
Mole fraction CO_2	89.0	84.3	%
Mole fraction H_2O	10.3	15.0	%
Mole fraction Ar	0.0	0.0	%
Mole fraction N_2	0.7	0.7	%

Table 13 shows that the composition of the rejected stream of carbon dioxide is similar for both of the cases with slightly higher amount of water in the rejected stream in Case 2. The carbon dioxide molar fractions were 89.0 % in Case 1 and 84.3 % in Case 2. From Table 13 it can be seen that the stream of rejected carbon dioxide from the process was 22.5 kg/s (81.0 t/h) for Case 1 and 23.1 kg/s (83.2 t/h) Case 2.

Finally, the state and composition of the non-condensable combustion gases after the addition of oxygen is presented in Table 14.

Table 14. *The state and composition of the non-condensable combustion gases after the addition of oxygen.*

	Case 1	Case 2	Unit
Temperature	53	40	ºC
Pressure	1	1	bar
Vapor fraction	1	1	-
Molar flow	5.2	8.6	kmol/s
Mass flow	204.2	337.8	kg/s
Mole fraction CO_2	72.2	20.5	%
Mole fraction H_2O	8.3	3.6	%
Mole fraction Ar	0.0	64.4	%
Mole fraction N_2	0.7	0.2	%
Mole fraction O_2	18.7	11.3	%

The transition to supercritical steam for the recirculation water occurs in the middle section of the HRSG. The recirculation water is already at a pressure higher than the critical pressure of water when it enters the middle section of the HRSG where it absorbs heat from the combustion gases and then passes the critical point of water and goes through the transition into supercritical steam. The transition of the recirculation water to supercritical steam for both cases is presented in Figure 27 and Figure 28 as a function of heat duty and temperature.

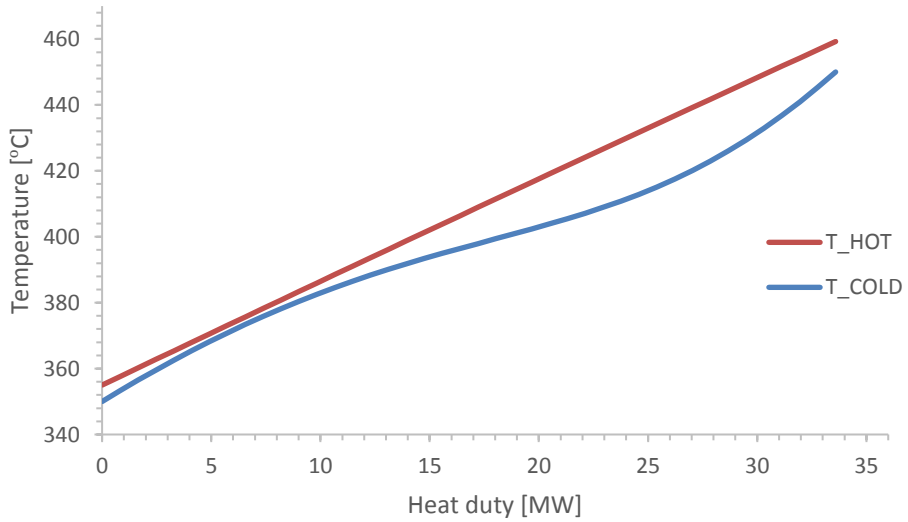

Figure 27. *Case 1: the transition to supercritical steam in the middle section of the HRSG. T_HOT depicts the combustion gases and T_COLD depicts the recirculation water. The recirculation water at pressure p = 300 bar.*

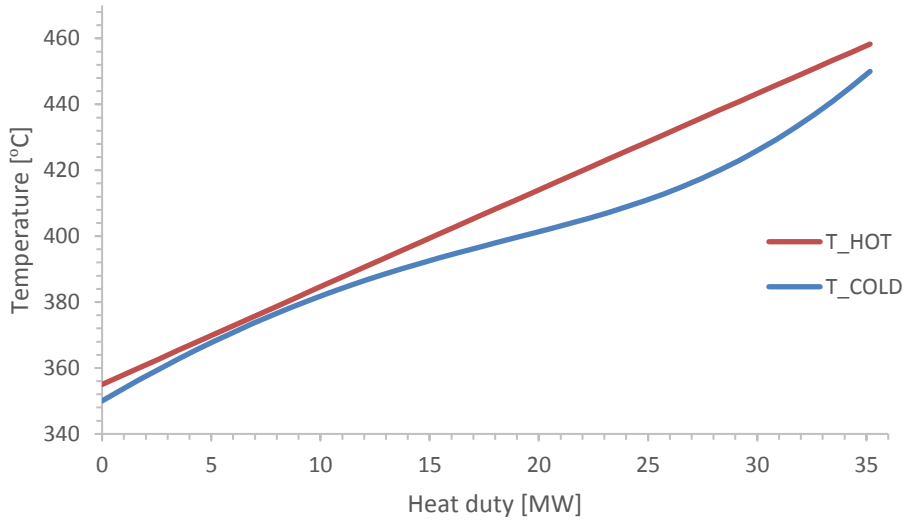

Figure 28. *Case 2: the transition to supercritical steam in the middle section of the HRSG. T_HOT depicts the combustion gases and T_COLD depicts the recirculation water. The recirculation water at pressure p = 300 bar.*

From Figure 27 and 28 it can be seen that the recirculation water behaves similarly in both cases and in a way that was expected and explained in Chapter 3.2 and can be seen in Figure 21. A transition from liquid water to steam would appear in a similar temperature-heat duty diagram as a straight vertical line that would lead to greater area between the hot and cold streams in the diagram. A smaller area between the hot and cold streams in the diagram is desired and can be achieved when working above the critical pressure of water, as can be seen from the Figures 27 and 28.

The intercooling used in the compression is not taken into consideration in detail but the heat duty and the reduction in temperature for the non-condensable combustion gases between each of the compression stage are presented in Table 15.

Table 15. *The effect of intercooling to the non-condensable combustion gases and heat duty between compressor stages.*

	Case 1	Case 2	Unit
Intercooler 1 heat duty	19.1	22.2	MW
Intercooler 1 temperature change	113	112	°C
Intercooler 2 heat duty	9.0	16.8	MW
Intercooler 2 temperature change	45	73	°C
Intercooler 3 heat duty	9.7	17.6	MW
Intercooler 3 temperature change	49	76	°C

Table 15 shows that more heat is rejected during intercooling in Case 2 and also the temperature difference is greater for Case 2 at intercooler 2 and intercooler 3. From Table 12 it can be seen that the mass flow in the compressors is higher for Case 2 and thus a higher amount of heat need to be rejected during the intercooling between the compression stages. Due to elemental properties of argon in the working fluid in Case 2 the fluid temperature rises more during compression leading to greater temperature difference during intercooling.

The work produced by the gas and steam turbines in the process can be found in Table 16. Also the net work produced by all the turbines is presented.

Table 16. *Work produced in the process for Case 1 and Case 2.*

Work produced	Case 1	Case 2	Unit
Gas turbine 1	297.2	299.4	MW
Gas turbine 2	8.2	35.1	MW
Steam turbine 1	9.7	13.2	MW
Steam turbine 2	13.4	13.9	MW
Net work produced	328.5	358.6	MW

The main clear difference between Case 1 and Case 2 is the work produced by the gas turbine 2 which results from the lower pressure ratio for the gas turbine 2 in Case 1. The work produced by gas turbine 1 is approximately the same in both cases but for a lower pressure ratio a higher mass flow through the gas turbine 1 is needed in Case 2. The work required by the compressors and pumps are presented in Table 17.

Table 17. *Work required in the process for Case 1 and Case 2.*

Work required	Case 1	Case 2	Unit
Compressor 1	25.7	27.1	MW
Compressor 2	11.9	19.8	MW
Compressor 3	12.4	20.6	MW
Compressor 4	33.1	57.7	MW
Pump 1	0.005	0.004	MW
Pump 2	1.2	1.3	MW
Net work required	84.3	126.5	MW

Compressor 1 was used to compress the working fluid to a pressure of 1 bar. From Table 17 it can be seen that the work required by compressor 1 is approximately the same in both cases, even though the compressor 1 inlet pressure is lower in Case 1 as can be seen from Table 9 but the mass flow through the compressor is higher in Case 2 as can be seen in Table 12. On the other hand, the compression ratio is the same for compressor 2, 3 and 4 in both cases which leads to higher amount of work required in Case 2 because of the higher working fluid mass flow.

The necessary oxygen inlet stream for both Case 1 and Case 2 as well as the cooling flow mass flows are presented in Table 18.

Table 18. *The oxygen inlet stream and the cooling flow mass flow.*

	Case 1	Case 2	Unit
Oxygen inlet stream	0.971	0.974	kmol/s
Oxygen inlet stream	31.082	31.164	kg/s
Cooling flow	470	438	kg/s

It is now possible to estimate the amount of energy needed for the oxygen production for the processes using the data from Table 18. 350 kJ of work per mass unit of oxygen has been suggested [21] so the energy required for oxygen supply equals to 10.9 MW in both Case 1 and Case 2.

For Case 2 the separation of carbon dioxide from argon needs to be estimated as well. When using the values from Table 11 and Table 12 and the equation (3.2) the required separation work equals to 1.7 MW. Air contains 0.93 molar-% of argon at standard conditions. [27] Argon is inserted into the process with the oxygen flow and it then accumulates into the process. In this study the oxygen flow was modelled as pure oxygen while the accumulation period of argon is not studied as the simulation was at steady-state condition. The carbon dioxide formed in the combustion that needs to be rejected from the system is separated from the non-condensable combustion gases consisting of mainly argon, carbon dioxide and steam so that the argon component remains circulating in the process. The separation process where carbon dioxide is separated from the non-condensable combustion gases is not studied in detail in this study but instead the separation work was estimated. The theoretical separation work that was used in this study to estimate the amount of work needed is 1.7 MW, which is not much compared to the net work produced by the process. Even though in practice the separation might require more work than estimated here, the theoretical separation work suggests only a minor loss of efficiency for the process because of the separation.

The process efficiencies are presented in Table 19. The heat energy Q_{in} added into the system is calculated from equation (5.7) and the thermal efficiency for the process is calculated according to equation (2.1). When the oxygen production and the separation of carbon dioxide from the mixture of mainly argon and carbon dioxide are taken into consideration, we get a net efficiency for the both cases. The net efficiency for the process is calculated from equation (2.3) where auxiliary work consists of the work required for oxygen production and the theoretical separation work.

Table 19. *The efficiencies of the process for Case 1 and Case 2.*

	Case 1	Case 2	Unit
Net work produced	328.5	358.6	MW
Net work required	84.3	126.5	MW
Fuel flow	7.925	7.946	kg/s
Qin	432.6	433.7	MW
Thermal efficiency	**0.565**	**0.535**	**-**
Oxygen production	10.9	10.9	MW
Separation work	0.0	1.7	MW
Net efficiency	**0.539**	**0.506**	**-**

The thermal efficiency of the process is 0.569 for Case 1 and 0.535 for Case 2. When oxygen production and the theoretical separation work for separating carbon dioxide from the argon-carbon dioxide mixture are taken into account in Case 2, the net efficiency of the process was calculated as 0.539 for Case 1 and 0.506 for Case 2. The difference between Case 1 and Case 2 is approximately 3 percentage points for both the thermal efficiency of the process and the net efficiency of the process. For both cases the effect of oxygen production is the decrease in the thermal efficiency by 3 percentage points, and for Case 2 the drop-off in efficiency due to the theoretical separation work is 0.4 percentage points.

A combined cycle process with oxyfuel combustion, called the Graz Cycle, that is in many ways similar to the process studied in this thesis was simulated in [25] by commercial simulation software IPSEpro. A more detailed presentation of the Graz Cycle can be found in [25]. The working fluid compositions after the main gas turbine are presented in Table 20 for the Graz Cycle and the two cases simulated in this thesis.

Table 20. *The working fluid composition after the main gas turbine. Values for Case 1 and Case 2 from Table 10 and values for the Graz Cycle from [25].*

	Case 1	Case 2	The Graz Cycle	Unit
Mole fraction CO_2	57.6	20.8	58.1	%
Mole fraction H_2O	41.9	27.9	41.2	%
Mole fraction Ar	0.0	51.1	0.0	%
Mole fraction N_2	0.5	0.2	0.2	%

From Table 20 it is notable that the working fluid composition after the main gas turbine is practically the same in Case 1 and in the Graz Cycle. Other main similarities and differences between the Graz Cycle and the two cases simulated in this thesis are presented in Table 21.

Table 21. *Comparison of the simulated cases and the Graz Cycle. The Graz Cycle values from [25].*

	Case 1	Case 2	The Graz Cycle	Unit
Fuel used	natural gas	natural gas	natural gas	-
Combustion pressure	20	20	40	bar
Turbine inlet temperature	1400	1400	1400	ºC
Main gas turbine pressure ratio	87.0	20.80	37.8	-
Condensation pressure	0.162	0.341	0.041	bar
Oxygen production	350	350	1225	kJ/kg
Thermal efficiency	**0.565**	**0.535**	**0.646**	-
Net efficiency	**0.539**	**0.506**	**0.548**	-

From Table 21 the main differences between the Graz Cycle and the cases simulated in this thesis can be seen. They include the combustion pressure, the main gas turbine pressure ratios, the condensation pressure, the oxygen production and the process efficiencies. The pressure ratios of the main gas turbine are clearly different between the Graz Cycle and the cases simulated in this thesis as is evident in Table 21. The pressure ratio is lower in the Graz Cycle than in Case 1, but the use of argon in Case 2 allows for the use of a pressure ratio that is approximately 55 % of the pressure ratio used in the Graz Cycle. For the Graz Cycle the oxygen production is estimated to require approximately 3.5 times more energy than in the cases simulated in this thesis. However, in the Graz Cycle the compression of oxygen to the combustion pressure is included in the oxygen production whereas in this thesis the oxygen is compressed to the combustion

pressure with the working fluid and therefore the compression of oxygen into combustion pressure was taken into account in the required compression work during simulation.

In Table 21 it is evident that there are major differences between the thermal efficiencies. The thermal efficiency of the Graz Cycle was calculated as 0.646 while in this thesis the thermal efficiencies were calculated as 0.565 for Case 1 and 0.535 for Case 2. The difference in the thermal efficiencies is 8.1 percentage points between the Graz Cycle and Case 1 and 11.1 percentage points between the Graz Cycle and Case 2. However, it needs to be noted that the major difference in the thermal efficiencies is at least partly due to the fact that in [25] the lower heating value of the fuel (46.465 MJ/kg) was used when calculating the thermal efficiency of the process whereas in this thesis the higher heating value of the fuel was used (54.584 MJ/kg) when calculating the thermal efficiency for both Case 1 and Case 2. As can be seen from equations (5.7) and (2.1), the difference between lower and higher heating value has a major effect on the thermal efficiency calculation. Also, the compression of oxygen to the combustion pressure is not taken into account in the thermal efficiency of the Graz Cycle but in the net efficiency instead. The differences in the way the thermal efficiency is calculated in the cases simulated in this thesis and for the Graz Cycle suggest that the process net efficiency is more usable when comparing the Graz cycle to Case 1 and Case 2 simulated in this thesis.

From Table 21 it can be seen that the Graz Cycle has a net efficiency of 0.548 while the net efficiency is 0.539 for Case 1 and 0.506 for Case 2. The difference is approximately 1 percentage point when compared to Case 1 and approximately 4 percentage points when compared to Case 2.

The results indicate that with the process studied in this thesis high process net efficiencies are achievable with both Case 1 and Case 2 as can be seen in Table 19 and with minimum irreversibility during heat transfer between the gas and steam turbine cycles of the combined cycle process as can be seen in Figures 27 and 28. Table 21 also shows that the results of the simulation in this thesis are comparable to previous research done with similar combined cycle process with carbon capture.

8. CONCLUSIONS

New ways of implementing the conventional combined cycle process for power generation could pave the way for efficiency increase that is important in the global battle against the rising temperatures worldwide and the Europe 2020 targets set by the EU considering energy efficiency. Carbon capture technologies on the other hand provide ways to control carbon dioxide emissions from conventional power generation methods as well as make way for newer, less polluting methods.

The concept of a combined cycle and the basics of gas and steam turbine cycles and carbon capture technologies were introduced in the beginning of the thesis. The latter part of the thesis consisted of studying and simulating a combined cycle process with oxyfuel combustion and carbon capture in steady-state conditions with Aspen Plus simulation software. The simulation was divided into two cases: Case 1 and Case 2. Case 1 was based on a novel configuration of the combined cycle characterized by oxyfuel combustion and effective carbon capture, as well as unconventional working fluids and the use of supercritical steam in the steam side of the combined cycle process. Case 2 was based on the same process as Case 1 with only minor differences. The purpose of Case 2 was to examine the effect of using argon in the working fluid of the process. Both Case 1 and Case 2 were simulated and optimized in order to maximize the thermal efficiency of the process in the chosen boundaries.

The study of a similar combined cycle process with oxyfuel combustion, the Graz Cycle, was found in the literature and its results were used as a comparison with the results from the simulation in this thesis. The simulation results showed that the thermal efficiency of the processes studied in this thesis was 0.565 in Case 1 and 0.535 in Case 2. The thermal efficiency of the Graz Cycle was 0.646 but it is notable that different calculation methods were used, most notably the fact that lower heating value was used instead of higher heating value, as well as different process configuration and process specifications. The oxygen production was not modelled as part of the simulation in this thesis but the amount of work needed to produce the necessary oxygen was estimated from the literature. It was estimated that 350 kJ for each mass unit of oxygen produced was required and this was taken into account when determining the process net efficiency. In addition, for Case 2 the energy required for the separation of carbon dioxide from the mixture of mainly argon and carbon dioxide was estimated by calculating the theoretical separation work for the mixture. When these auxiliary energy requirements were taken into account the net efficiency of the studied process was determined as 0.539 in Case 1 and 0.506 in Case 2. The Graz Cycle was found to have a net efficiency of 0.548.

In addition to studying the performance of the process, the two-case approach enabled the comparison of the effect of two different working fluid compositions for the process. One

of the major differences between the cases was the pressure ratio for the main gas turbine. For the same turbine inlet pressure the pressure ratio of the main gas turbine was 87.0 in Case 1 compared to 20.8 in Case 2. As the inlet pressure was the same in both cases, the difference in the pressure ratios was due to a lower discharge pressure in Case 1. The pressure ratio of the main gas turbine in the Graz Cycle was 37.8.

The discharge pressure for the main gas turbine was 0.230 bar in Case 1 and 0.963 in Case 2. The lower pressure ratio and higher discharge pressure results in lower capital costs concerning the main gas turbine in Case 2, especially so as the diameter of the turbine blades increase towards the low pressure end of the turbine further increasing the size of the turbine. Another advantage of the higher discharge pressure for the main turbine in Case 2 is that it leads to lower capital costs concerning the gas side of the HRSG because of the smaller temperature difference between the gas side of the HRSG and environment. However, the difference in both thermal and net efficiencies of the process was approximately 3 percentage points in favor of Case 1. Thus a more detailed economic analysis would be needed to decide which one of the two cases simulated in this thesis could provide the best overall results in practice.

The storage and after treatment of the rejected carbon dioxide was not taken into account in detail in this study. The stream of rejected carbon dioxide from the process was 81.0 t/h for Case 1 and 83.2 t/h for Case 2 with carbon dioxide molar fractions of 89.0 % and 84.3 % for Case 1 and Case 2, respectively.

The simulation results indicate that the simulated combined cycle process allows for effective carbon capture while maintaining high process efficiency and minimum irreversibility during heat transfer between the gas and steam turbine cycles of the studied combined cycle process. The Graz Cycle used for comparison has a slightly higher net efficiency than either of the cases studied in this thesis. However, the effect of the differences in the process configuration and process specifications between the Graz Cycle and the two simulated cases studied in this thesis are not clear.

The separation of carbon dioxide from a mixture mainly consisting of carbon dioxide and argon needs more research but it is likely that the effect of the separation to overall efficiency of the process remains small as indicated by the theoretical separation work used in the simulation. A more complete economic analysis of the process studied in this thesis and a demo-scale plant are recommended to verify the results and confirm the economic feasibility of the process as well as make it possible to find out which one of the two cases simulated in this thesis could provide more cost-effective results in practice.

REFERENCES

[1] Europe 2020 indicators – climate change and energy, Eurostat, Available (accessed on 28.9.2016): http://ec.europa.eu/eurostat/statistics-explained/index.php/Europe_2020_indicators_-_climate_change_and_energy

[2] 2030 Energy Strategy, European Comission, Available (accessed on 28.9.2016): http://ec.europa.eu/energy/en/topics/energy-strategy/2030-energy-strategy

[3] R. Stanger, T. Wall, R. Spörl, M. Paneru, S. Grathwohl, M. Weidmann, G. Scheffknecht, D. McDonald, K. Myöhänen, J. Ritvanen, S. Rauhala, T. Hyppänen, J. Mletzko, A. Kather, S. Santos, Oxyfuel Combustion for CO_2 Capture in Power Plants, International Journal of Greenhouse Gas Control, Vol. 40, 2015, pp. 55-125

[4] N. Petchers, Combined Heating, Cooling & Power Handbook – Technologies and Applications (2nd Edition), Fairmont Press, Inc., 2012

[5] G.F.M de Souza (Ed.), Thermal Power Plant Performance Analysis, Springer, 2012

[6] R. Raiko & Katriina Kirvelä. (2013). ENER-8010 Energiatekniikan perusteet. Lecture notes 2013. Tampere University of Technology. 184 p.

[7] A.D. Rao, Combined Cycle Systems for Near-Zero Emission for Power Generation, Woodhead Publishing Limited, 2012

[8] Gas Turbine for Power Generation: Introduction, Available (accessed on 23.9.2016): http://www.wartsila.com/energy/learning-center/technical-comparisons/gas-turbine-for-power-generation-introduction

[9] R. Raiko. (2013). KEB-43200 Voimalaitostekniikka. Lecture notes 2013. Tampere Univeristy of Technology. 248 p.

[10] M.P. Boyce, Gas Turbine Engineering Handbook (3rd Edition), Elsevier, 2006

[11] P. Breeze, Power Generation Technologies (2nd Edition), Elsevier, 2014

[12] R. Raiko & I. Saarenpää. (2014). KEB-43100 Höyrytekniikka. Lecture notes 2014. Tampere University of Technology. 254p.

[13] Siemens Steam Turbine SST-6000 series, Available (accessed on 23.9.2016): http://www.energy.siemens.com/hq/en/fossil-power-generation/steam-turbines/sst-6000.htm#content=Description

[14] Steam Turbine and Generators brochure, Available (accessed on 23.9.2016): http://www.doosanskodapower.com/en/steam/supercriticalparameters.do

[15] R Kehlhofer, F. Hannemann, B. Rukes, F. Stirnimann, Combined-Cycle Gas and Steam Turbine Power Plants (3rd Edition), PennWell Books, 2009

[16] M. Nurmia, Patent application 20155653, Brayton-Rankine with carbon capture, applied: 11.09.2015

[17] B. Liu, K. Chien, C. Wang, Effect of Working Fluids on Organic Rankine Cycle for Waste Heat Recovery, Journal of Energy, Vol. 29, 2004, pp. 1207-1217

[18] Critical point (thermodynamics), Wikipedia, Available (accessed on 26.9.2016): https://en.wikipedia.org/wiki/Critical_point_%28thermodynamics%29

[19] S.A. Rackley, Carbon Capture and Storage, Elsevier, 2010

[20] A.R. Smith, J. Klosek ,A Review of Air Separation Technologies and Their Integration with Energy Conversion Processes, Fuel Processing Technology, Vol. 70, 2001, pp. 115-134

[21] M. Raiko, Evaluation of a Novel Cryogenic Oxygen Enrichment Method, Master's Thesis, Tampere University of Technology, 2015

[22] Aspen Plus Help files

[23] D. Peng, D.B. Robinson, A New Two-Constant Equation of State, Industrial & Engineering Chemistry Fundamentals, Vol. 15, 1976, pp. 59-64

[24] Acentric factor, Wikipedia, Available (accessed on 19.10.2016): https://en.wikipedia.org/wiki/Acentric_factor

[25] W. Sanz, H. Jericha, F. Luckel, E. Göttlich, F. Heitmeir, A Further Step Towards a Graz Cycle Power Plant for CO_2 Capture, Proceedings of GT 2005 ASME Turbo Expo 2005: Power for Land, Sea and Air, Reno-Tahoe, Nevada, USA, June 6-9, 2005

[26] H.J. Yang, D.W. Kang, J.H. Ahn, Evaluation of Design Performance of the Semi-Closed Oxy-Fuel Combustion Combined Cycle, Journal of Engineering for Gas Turbines and Power, Vol. 134, 2012

[27] Air composition, The Engineering Toolbox, Available (accessed on 27.9.2016): http://www.engineeringtoolbox.com/air-composition-d_212.html